– 9 –

Solid State Physics

Solids are mostly subdivided into crystal and amorphous substances. In this chapter the crystalline state is predominantly considered although some features of the amorphous and liquid states will also be briefly touched on.

9.1 CRYSTAL STRUCTURE, CRYSTAL LATTICE

A crystal is characterized by a three-dimensional, regular, periodic array of particles—atoms and/or molecules. Modern experimental techniques allow us to see the structure of large molecules in crystals using an electron microscope. Figure 9.1 is an electron photograph of a crystal of tobacco mosaic virus, showing the regular packing of the molecules in a crystal.

Remember that by "molecule" we usually mean the smallest part of a substance that can exist alone and retain the characteristics of that substance. Imagine that we can divide a crystal until it becomes the "brick," which retains the main (but, certainly, not all) characteristics of the whole crystal. The contents and form of this "brick" defines the crystal structure: the relative amount and mutual disposition of atoms (molecules), the chemical composition of crystalline material, the interatomic distances and valence angles (i.e., chemical bonding), etc. The smallest part of the crystal that retains the specified characteristics (the "brick") is referred to as a unit cell. Using the property of periodicity one can build the whole crystal by regular repetition of unit cells along coordinate axes, as shown in Figure 9.2.

A crystal can be characterized both by the unit cell (the carrier of the chemical composition and atomic structure), and by three translation vectors $\boldsymbol{a}$, $\boldsymbol{b}$ and $\boldsymbol{c}$; the latter can be used to build the whole crystal from original cells. Each of these three vectors corresponds to a symmetry operation, since these operations superpose a crystal with itself: each atom (supposed to be a point) moves over to a similar atom in the nearby unit cell. Any point (atom, including) can be transferred to another crystal point, identical to the first, by operation of a translation $\mathbf{t}$, which is

$$\mathbf{t} = m\boldsymbol{a} + n\boldsymbol{b} + p\boldsymbol{c}, \tag{9.1.1}$$

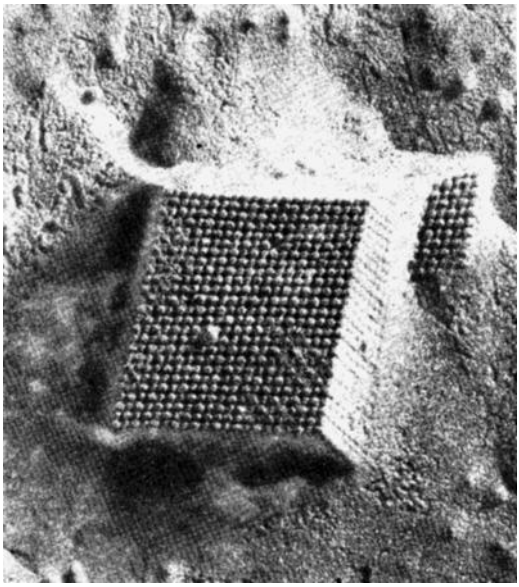

Figure 9.1 Image of the tobacco mosaic crystal as seen in the electron microscope (size of molecules is approximately 25 nm).

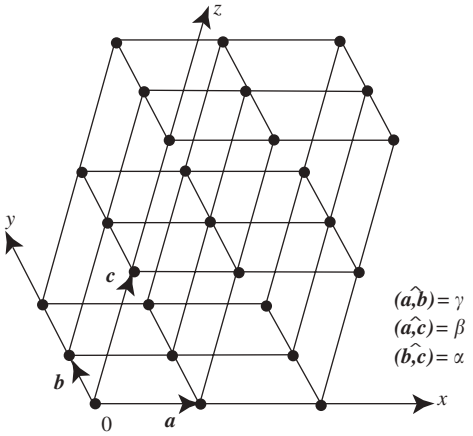

Figure 9.2 Crystal lattice: a unit cell based on $\boldsymbol{a}$, $\boldsymbol{b}$, $\boldsymbol{c}$ vectors and the crystal build-up.

where m, n and p are integers which number the unit cell to which the translation is taking place.

Unlike the symmetry elements considered in Section 1.3.7, translation is an attribute of the crystalline state, because it translates a given atom to a similar one in the neighboring unit cell, but does not combine an atom with itself. It is important to note that the crystal

is here considered to be of infinite size; this is a good approximation, since crystal size is usually many orders of value larger than the unit cell.

The system of translations forms a so-called crystal lattice; this presents a mathematical abstraction: describing the translational characteristics of a given crystal. In Figure 9.2 this position is illustrated. Vectors $\boldsymbol{a}$, $\boldsymbol{b}$ and $\boldsymbol{c}$ represent a set of three translations in three dimensions, which together with angles α, β and γ, define the form and size of the unit cell. The crystallographic axes x, y and z are usually directed along the main translations. Note that the choice of three main translations is ambiguous, there exist certain rules to make this choice but this is not important here. The cross points of the axes are called lattice nodes.

It should once again be emphasized that while the crystal structure is the arrangement of atoms in the crystal, the crystal lattice is a system of translations, describing the translational properties of the crystal.

The form of cells, the location of atoms in them and, accordingly, the crystal's physical properties are defined by the symmetry laws. All these comprise the subject of crystal physics and crystal chemistry.

Correlations between the translation vector length and the angles between them define possible crystal classes or syngony, resulting from the unit cell form and the crystal lattice. There are seven crystal classes (or syngony), plotted in Table 9.1.

The position of origin is chosen from considerations of rationality. So, in Figure 9.3 the atomic structure and crystal lattice of a Cl_2 crystal is depicted: the origin is chosen not in the position of an atom, but in the CM of the Cl_2 molecule. (In this instance a crystal node is in "emptiness.") Planes drawn through the nodes (but not in general through atoms) are called crystallographic planes (see Section 6.3.5).

A lattice node is defined by its coordinates (in the units of the vector length), which are placed in double square parentheses (for instance, [[001]]). All parallel directions in a crystal are equivalent. So a straight crystal line (or simply line) is conducted through the origin and its indexes are defined by the coordinate of the first node, lying on this line; a line's indexes are enclosed in brackets (so, direction [001] complies with the direction to axis z, since the first node on it has the coordinates [[001]]).

Table 9.1

The crystal classes (syngony)

Syngony	Relations between lattice periods	Relations between angles
Triclinic	$a \neq b \neq c$	$\alpha \neq \beta \neq \gamma$
Monoclinic	$a \neq b \neq c$	$\alpha = \beta = 90° \neq \gamma$
Orthorhombic	$a \neq b \neq c$	$\alpha = \beta = \gamma = 90°$
Tetragonal	$a = b \neq c$	$\alpha = \beta = \gamma = 90°$
Trigonal (rhombohedral)	$a = b = c$	$\alpha = \beta = \gamma \neq 90°$
Hexagonal	$a = b \neq c$	$\alpha = \beta = 90°, \gamma = 120°$
Cubic	$a = b = c$	$\alpha = \beta = \gamma = 90°$

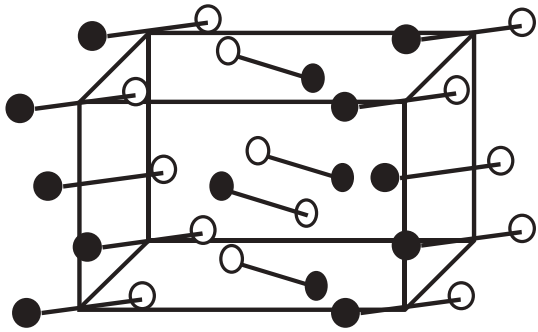

Figure 9.3 Crystal unit cell of Cl_2: there is an arbitrary rule in the choice on the unit cell.

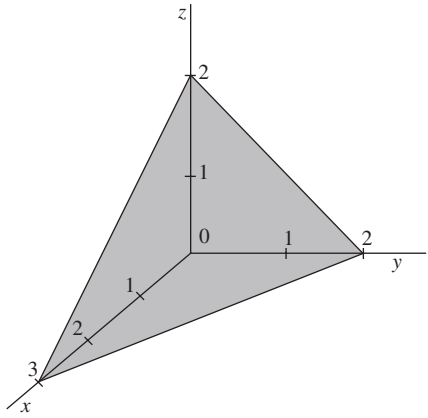

Figure 9.4 An order of the Miller indexes determination.

The family of parallel crystallographic planes is defined by three indexes h, k, l called the Miller indexes. The indexes are inversely proportional to the segments cut by the given plane on the axes, provided it is the nearest plane to the origin; they are bracketed in parentheses. Let a plane cut definite segments on the axes. In Figure 9.4 such lengths (in units a, b and c) are 3,2,2. (These lengths in unit cell periods can be whole or fractional numbers.) They must be "turned over" and multiplied by a single whole number (here the number is 6) to make them whole numbers $\left[\left(\frac{1}{3}, \frac{1}{2}, \frac{1}{2}\right) \rightarrow (2,3,3)\right]$. The three whole numbers obtained (2,3,3) are the Miller indexes of this plane. If a plane cuts an axis on the negative side of the origin, the corresponding index is negative indicated by placing a minus sign above the corresponding index (e.g., $\bar{h}$,k, l). In Figure 9.5 an example of some crystallographic planes in a cubic lattice is presented. Index zero amongst the Miller indexes corresponds to the fact that a plane cuts on the corresponding axis a segment equal to infinity, i.e., this plane is parallel to a given axis. If there are two zeroes amongst the indexes it means that a given plane is parallel to the corresponding unit cell edge.

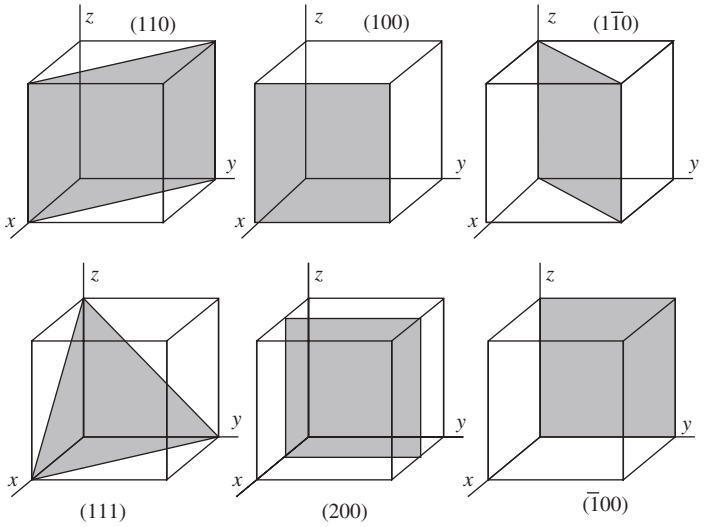

Figure 9.5 Selected crystallographic planes in a cubic crystal.

The correlation presented describes the so-called primitive cells in which there is only one atom (each atom in the nodes belongs simultaneously to eight cells, which gives for one unit cell $8 \times (1/8) = 1$ atom). The unit cell of each crystallographic class is characterized by a definite symmetry corresponding to the crystal space symmetry. It is possible to place an additional atom in a primitive cell in such a manner that the cell symmetry does not change. For instance, in the cubic primitive cell one can introduce an additional atom into the cell's center $\left[\left[\frac{1}{2},\frac{1}{2},\frac{1}{2}\right]\right]$ without destroying its symmetry. A body-centered lattice (BCC) with two atoms to the cell is obtained. Iron crystals, for instance, possess such a structure. It is possible to place atoms at the centers of the edges of a primitive cell $\left[\left[\frac{1}{2}\,\frac{1}{2}0\right]\right]$, $\left[\left[\frac{1}{2}0\frac{1}{2}\right]\right]$ and $\left[\left[0\frac{1}{2}\,\frac{1}{2}\right]\right]$ preserving the cubic symmetry. In a similar manner, the so-called face-centered cubic (FCC) with four atoms in the unit cell is obtained. Copper, for instance, has a FCC structure. Such cells are called cells with basis (or Bravais lattices).

Crystallographic directions are characterized by identity distances (periods), i.e., the shortest distance between identical atoms in a given direction. Parallel crystallographic planes are also identical to each other. The distance between two adjacent planes with indexes h, k, l, or what amounts to the same things, the distance from the origin to the nearest crystallographic plane with the same indexes are called interplanar spacing $d_{h,k,l}$. Exactly this value falls into the Bragg equation (refer to Sections 6.3.5).

Periods of lattices a, b, c together with angles α, β, γ, plane indexes (h, k, l) and interplanar spacing d are bound by a so-called quadratic form. For the simplest case of a cubic crystal, the quadratic form is presented by the equation

$$\frac{1}{d^2} = \frac{h^2 + k^2 + l^2}{a^2}. \tag{9.1.2}$$

Structure and crystal lattice define the positions of atomic CM in the unit cell. In addition, atoms in crystals perform thermal oscillations, significantly influencing the crystal's physical properties. These oscillations are characterized by root mean square displacements.

The main method of crystal structure determination is X-ray diffraction analysis (refer to Section 6.3.5). Experiments that use small single crystals and/or polycrystalline samples allow one to determine the mutual location of atoms in crystals of rather complex chemical compounds (for instance, a thousand or more atoms in the unit cell) together with the nature and parameters of atomic thermal vibrations (their root mean square displacement values). For investigation of special questions, methods of neutron and electron diffraction are also used (refer to Chapter 7.2).

EXAMPLE E9.1

Knowing the density of a Ca single crystal $\rho = 1.55 \times 10^3$ kg/m^3 determine: (1) the lattice period a; and (2) the closest interatomic distance d. The Ca crystal is of the FCC structure type.

Solution: The unit cell volume V of a cubic crystal can be bounded with the lattice period a by a simple expression $V = a^3$. On the other side, it can be expressed as a ratio of the molar volume to the number of unit cells in one mole of the crystal $a^3 = V_m/Z_m$*. The molar volume V_m is $V_m = M/\rho$. The number of the unit cells in one mole is $Z_m = N_A/n$ where n is the number of atoms in the unit cell. Substituting these values into * we obtain $a^3 = nM / \rho N_A$ wherefrom $a = \sqrt[3]{(nM / \rho N_A)}$. Taking into account the number of atoms in the FCC unit cell (Chapter 9.1) we arrive at $a = 556$ pm.

(2). The closest interatomic distance in the FCC lattice is the face diagonal $d = a\sqrt{2}/2$. Therefore, d can be found $d = 393$ pm, where the atomic radius can be calculated from $r = (d/2) = 1.81$ Å.

EXAMPLE E9.2

Write down the indexes of crystallographic directions presented in Figure E9.2 by a bold line (refer to Chapter 9.1).

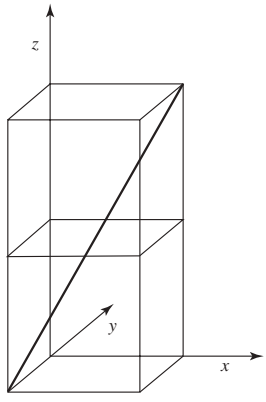

Solution: The crystallographic direction does not cross the origin (axes symbols without asterisks). However, we know that all the nodes of a crystal lattice are equivalent. Therefore, we can shift the origin in the point [[100]] in the figure. This point is the new origin. Then the line will cross the node [[$\bar{1}$01]]. These are the indexes of the direction [$\bar{1}$01].

EXAMPLE E9.3

In Figure E9.3 a crystal lattice is presented. Write down indexes of the crystallographic plane crossing three nodes indicated in the figure.

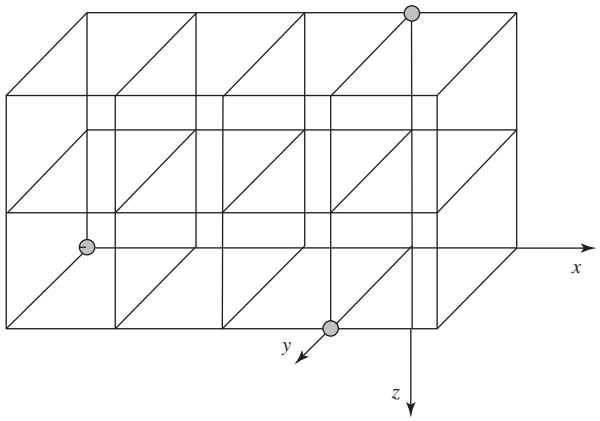

Solution: It can be seen from the Figure E9.3 that points cut on coordinate axes (in periods units) are $x = -3$, $y = 1$ and $z = -2$. According the rule we should obtain the reciprocal values; they are $\left(\frac{\bar{1}}{3}, 1, \frac{\bar{1}}{2}\right)$. Multiply the three value on 6 we arrive at ($\bar{2}$, 6, $\bar{3}$). Note that indexes can be multiplied by a constant value, including negative. All planes obtained will be identical.

9.2 ELECTRONS IN CRYSTALS

9.2.1 Energy band formation

In Chapter 7 the electron structure of free atoms, i.e., not subjected to any external influences, was considered. In a crystalline state the distance between the atoms is comparable with their size; so each of them appears strongly influenced by its neighbors. The interatomic interaction and periodic character of a crystal field render an extremely strong

influence on the atomic ensemble. As a result, crystals possess a complex of the properties strongly distinguishing them from ensembles of free atoms.

Let us consider the essence of the process using the example of the hydrogen-like atom of sodium with 11 electrons in its shell in a free state. In Figure 9.6 (above) a potential electron energy curve of two neighboring atoms in a field of their nuclei is presented. All levels of energy up to 2p are occupied completely though there is one noncoupled electron in the outer 3s level. The potential curves go up to $U = 0$ but are not overlapping. Each electron is fixed near its nucleus.

The same picture is presented in Figure 9.6 (below); however, here the distance between atoms corresponds to the shortest interatomic distance in sodium metal ($a = 4.3$ Å). Firstly, the potential curves in a crystal form a unique periodic potential with the maxima located appreciably below the zero level of energy. Secondly, an upper occupied 3s-electron level has risen above the potential barriers and a corresponding electron appears capable of moving along the whole crystal. It is usually said that collectivization of valence electrons has occurred. Such collectivized electrons form an ensemble of quasi-particles that has lost part of their initial properties (see Section 9.2.2). The overlapping of the outer 3s orbits has occurred.

On approach, changes also touch the inner electrons. The mutual influence of atoms transforms the very "thin" electron's levels into a band of final width. In Figure 9.7a scheme of such level expansion is given for several crystals. In Figure 9.7a the 1s level of a lithium atom is expanded insignificantly whereas the 2s level has formed a rather wide

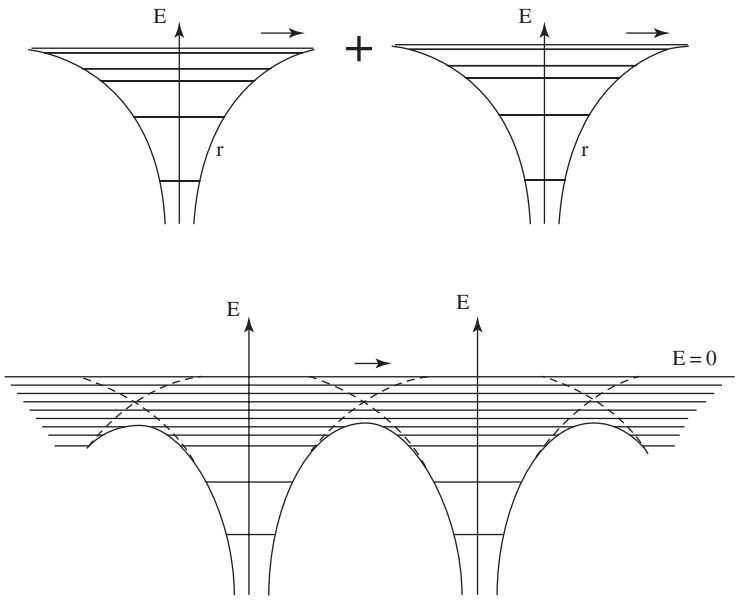

Figure 9.6 Interaction of two sodium atoms. *above* – the initial state, the potential curves of the two free atoms not interacting to each other, *below* – overlapping of the upper electron shells at the interatomic distance became closer reduced to that in metallic sodium: this give rise to Bloch's free electron formation.

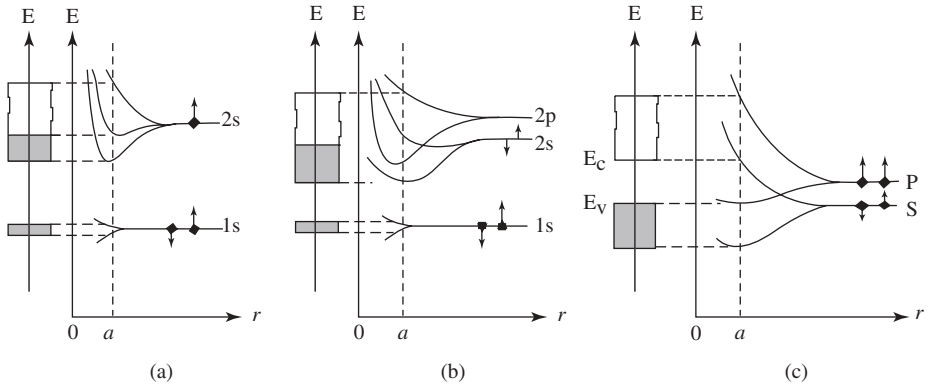

Figure 9.7 Broadening of the electron's energy levels and formation of energy bands: (a) lithium crystal (in the 2s band part of the level is occupied, this is shaded in a section, whereas other part remains free), (b) bands in beryllium, (c) bands in diamond-like crystals.

2s band. In a beryllium crystal (Figure 9.7b), 2s and 2p levels have formed an overlapping band. This mixed band is called a *hybrid band*. In diamond-like crystals with strongly pronounced covalency the bands were split in two (Figure 9.7c); each of them contains four states for one atom: one s-state and three p-states. These bands are subdivided by the *forbidden* energy band. The lower occupied band is referred to as a *valence* band, and the upper band as a *conductivity* band.

The picture described corresponds to the so-called strong-binding approximation. In a weak-binding approximation the electron behavior in a periodic crystal field is considered. For the analysis of the latter case it is necessary to solve the Schrödinger equation for a particle moving in a periodic field F. Bloch has offered a function consisting of the product of two functions:

$$U(x) = u(x) \times e^{ikx}, \tag{9.2.1}$$

The function $u(x)$ describes the electronic potential of a single atom and the other (exponential) ensures the periodicity $u(x + a) = u(x)$. This function is called the Bloch function. Such potential should be substituted into the Schrödinger equation and the allowed values of energy can be derived. Instead of a smooth parabolic function $E = (\hbar^2 / 2m)k^2$ a curve with breaks is derived.

Some representation of the physical origin of such breaks can be given using diffraction electron properties (see Section 7.1): breaks occur at values k, corresponding to back reflection according to Bragg's equation (6.3.11). Back reflection in this case can take place when an angle θ is 90° and, accordingly, $n\lambda = 2d$ (n is an integer designating the order of reflection). Remembering that $\lambda = 2\pi/k$ the equation can be presented as

$$k = \frac{n\pi}{d}, \tag{9.2.2}$$

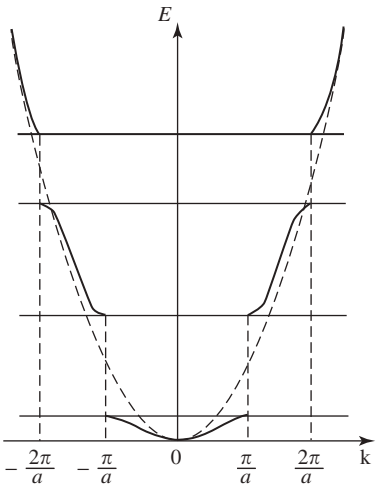

Figure 9.8 Electron energy E as a function of the wavenumber k. The same curve for a free atom is presented by a broken curve.

where d is the interplanar distance. If the planes (h00) are considered, the interplanar distance is a and eq. (9.2.2) appears in the form

$$k = \frac{n\pi}{a}. \tag{9.2.3}$$

As a result the curve $E(k)$ looks like that given in Figure 9.8: on a background of classical parabolic dependence in the places determined by expression (9.2.3) the curve has breaks. The forbidden energy gap, which we met above, is formed. We are unable now to call the particles as electrons; we must call them *quasi-particles* (*quasi-electrons*).

The properties of a quasi-particle with a wavenumber k close to $n\pi/a$ (at the bottom or near the top of a band), differ appreciably from the properties of really free electrons. In particular, their effective mass m^* differs at the "top" and "bottom" of the energy band. It follows from this fact that m^* is defined by the second derivative of an energy E on wave vector k, i.e., $m^* = (d^2E/dk^2)$; from the curve it can be seen that m^* depends on k and can even change sign.

9.2.2 Elements of quantum statistics

Because of mutual influence, some atomic electrons are generalized forming a "gas" of quasi-electrons in crystals. These electrons preserve some properties of free electrons (e.g., each of them possesses a classical momentum) but, at the same time, also possess properties that distinguish them from really free particles (e.g., they have a mass different from the classical electron mass). Some well-known electric properties of metals are caused by this "gas." However, it appears that in a model of free "electron gas" theoretical calculations strongly overestimate experimentally known characteristics; only a small part of the generalized electrons can take part in the formation of these properties.

Are these electrons indeed the gas of free electrons? The answer to this question has already been obtained: no, there are no free electrons in metals; electrons form energy bands that can either be overlapping, or be separated by the forbidden energy gap. Besides, moving in a periodic crystal field, electrons are symmetry-dependent. It is necessary to answer one more question: how are electrons distributed among these bands and how are they distributed inside the band?

In classical Newtonian physics the elementar volume of a configurational space cell is infinitesimal (it looks like Planck's constant $\hbar$ is accepted to be zero); the electron distribution upon their energy is given by Maxwell–Boltzmann statistics: there are large amounts of particles, all of which tend to occupy the state with the lowest energy, though chaotic temperature motion, on the other hand, scatters them on different energies. This process is described by the Boltzmann factor.

In quantum physics the volume of a phase space cell is no smaller than h^3 because of the uncertainty principle; the number of cells is limited accordingly and this leads to the limited amount of energy levels in the bands. The problem of particle distribution among cells (and energy levels) is not apparent. Regulation is given by quantum statistics. The energy spectrum is presented by energy bands with limited "capacities."

Consider the energy structure of a valence band. The example of sodium atom was given above; every atom from its 11 electrons delivers only 1 to the valence band; besides, every atom "brings" one level to each energy band; levels regularly fill the band, they cannot overlap since the uncertainty principle and exclusion principle do not permit overlapping. If we assume that sodium crystal comprises N atoms, the conduction band is half-filled because of the spin degeneration. How are these electrons distributed on the levels? Figure 9.9 presents such a half-filled band. The upper occupied level at 0 K is referred to as the *Fermi-level* (E_F); energy counts up from the bottom of the band. The same is presented in Figure 10a; the graph $f(E)$ forms a step, all levels under E_F are occupied whereas all levels over E_F are empty.

It is suggested in quantum statistics that particles with half-integer spin obey Fermi–Dirac statistics; such particles are called *fermions*. Electrons have a spin quantum number equal to 1/2 and therefore are fermions and must obey Fermi–Dirac statistics.

The mathematical description of Fermi–Dirac statistics is given by the Fermi distribution function

$$f(E) = \left[e^{(E-E_F)/(\kappa T)} + 1\right]^{-1}. \tag{9.2.4}$$

The magnitude of this function depends on the sign of difference $E - E_F$. At 0 K and $E < E_F$ the difference is negative and $f(E) = 1$. At $E > E_F$ the difference is positive and $f(E) = 0$. This corresponds to the fact that up to Fermi energy, all levels are occupied by electrons according to Pauli's exclusion principle. When the temperature increases, only those electrons close to the E_F level transmit to higher levels (Figures 9.9 and 9.10b) and take part in excitation. The number of such electrons is proportional to κT, as is shown in the figure. The point is that only such electrons can participate in electric properties. At $\kappa T >> E_F$ function $f(E)$ corresponds to nondegenerated gas and Fermi–Dirac distribution transforms to Boltzmann distribution. However, this can happen only at very high temperatures when the crystal hardly exists.

At absolute zero temperature all levels are occupied by electrons up to E_F. When temperature increases some of the electrons are excited and occupy free levels of energy. These electrons define the electron conductivity of metals. The average energy width of this "excitation band" is equal to κT, as is marked in Figures 9.9 and 9.10.The opposite case is presented by particles with integer spin, in particular photons with a spin quantum number 1. Such particles are referred to as *bozons* (Bose particle). They obey Bose–Einstein statistics. A distribution function $f(E)$ for bozons is expressed as

$$f(E) = \left[e^{(E-\mu)/(\kappa T)} - 1\right]^{-1}. \tag{9.2.5}$$

The value μ in this equation is the so-called chemical potential, i.e., the thermodynamic function of a system, which is determined by the system energy change at the change of the particle number by 1.

A feature of photon gas is the fact that, at first, photon gas cannot exist by itself: a source of photons as heated body surface is necessary for its maintenance. Further, all photons in vacuum move at an identical speed equal to the speed of light c and possess energy $\hbar\omega$, momentum $\hbar\omega/c$ and mass E/c^2 (refer to Section 1.6). They cannot stop; their resting mass is zero. Moreover, photons do not collide with each other and their equilibrium is achieved only on interaction with heated surfaces; therefore their quantity is not fixed, it is established by the equilibrium with the heated body.

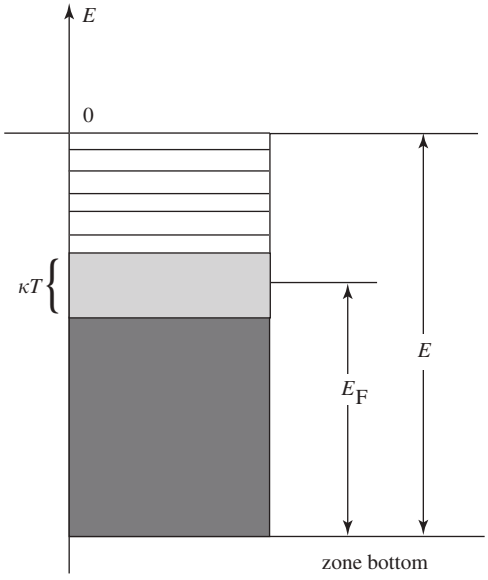

Figure 9.9 An energy band structure. E is the total depth of the band, E_F is the Fermi energy count from the band bottom. Schematically the dark field presents the fully occupied by electrons band at zero temperature, non-occupied levels space is white, a variable part of a band of κT in width is active, i.e., can be exited and participate in conductivity. The energy levels are very close to each other and therefore are not shown in the diagram.

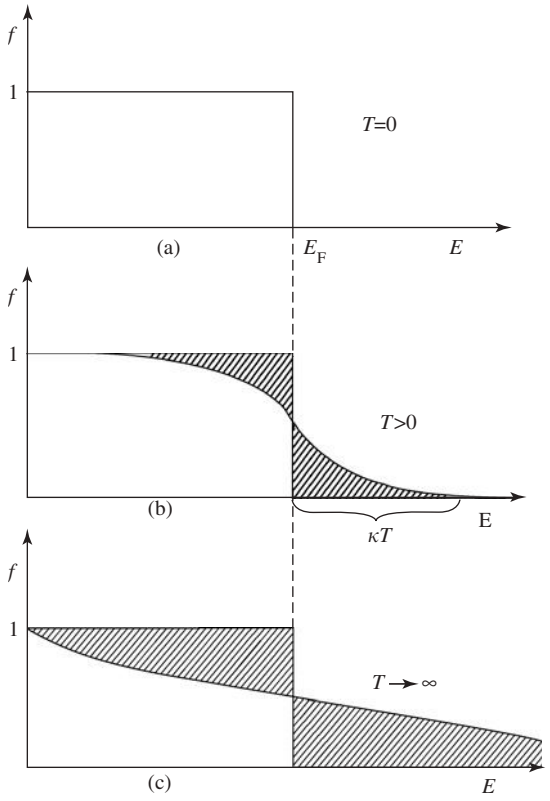

Figure 9.10 The graph of Fermi-Dirac distribution: (a) at 0 K it looks like a step, (b) at intermediate temperature, the border near Fermi energy is fuzzy. (c) at $T \to \infty$ the distribution transforms to Boltzmann law.

An electron with half-integer spin is a fermion, i.e., it has to obey Fermi–Dirac statistics. All the usual metal electroconductivity properties are in agreement with these statistics. However, in some cases two electrons can produce the so-called Cooper's pairs with compensated spin, the spin of the Cooper pairs is zero. Therefore, such pairs transform electrons from fermions to bozons. There are no Pauli's exclusion principles for bozons; they can be "condensed," i.e., they occupy all the levels, and nearly all participate in electroconductivity. Superconductivity can then take place.

This suggestion theoretically explains the metal and intermetallic compound superconductivity phenomenon (J. Bardin, L.N. Cooper and R. Schrieffer, Nobel Prize 1972), discovered earlier by H. Kamerling-Onnes (Nobel Prize, 1913). This phenomenon occurs only at very low temperatures ($\approx$20 K). However, superconductivity has been discovered in nonmetallic, oxide-type chemical compounds with critical points of superconductivity up to $\approx$140 K (in liquid nitrogen region) (so-called high-temperature super conductors, HTSC) (J.G. Bednorz and K.A. Muller, Nobel Prize, 1987). Intensive attempts to synthesize new materials of this kind are in progress.

9.2.3 Band theory of solids

Band theory relates to the electrical properties of solids and the character of their energy bands. The corresponding relation is given in Figure 9.11. The case of metallic sodium already examined above is presented in Figure 9.11a. Electrons fully occupy the 2p band, but the conducting 3s band is half-filled. Therefore, 2p electrons do not participate in conductivity but the electrons lying near E_F in the 3s band can easily be excited by an external electrical field and take part in an electrical current. Consequently, sodium, like all other alkali metals, is a conductor. This situation is shown in Figure 9.11b, where a scheme of another case of a conductivity band created both by 3p- and 3s-electrons is depicted.

Another picture of energy band filling is shown in Figure 9.11c. It corresponds to full occupation of a valence band (E_F equals the band top energy) with the presence of the forbidden energy gap E_g between the valence band and the band of conductivity. Electrons of the valence band cannot be so easily excited now by the action of an inner field to take part in conductivity (for this, electrons have to be transmitted to the conduction band, overcoming a broad energy gap); the corresponding materials possess a dielectric property. If the gap is narrow in comparison to κT, the material is an intrinsic semiconductor (Figure 9.11d).

In addition, there exist two great classes of semiconductors characterized by the presence of local energy levels (to the account of different admixtures) in the forbidden energy gap. If these levels lie close to the top of the valence band (Figure 9.12a) (this is called the acceptor level), electrons of the valence band occupy them and release some levels in this band. The so-called hole conduction appears (on account of vacancies near the top of the valence band). Such materials are semiconductors of p-type. Germanium crystals with indium admixture can be numbered amongst them.

If occupied local electron energy levels are near the bottom of an empty conduction band they can be excited directly to this band (Figure 9.12b). Such levels are called donor levels and the material is a semiconductor of n-type (germanium with the admixture of arsenic). In intrinsic semiconductors (for instance, pure germanium and silicon) the local levels are absent; however electrical conductivity appears because of the narrowness of the forbidden gap and at moderately high temperature an excitation of electrons from the valence band directly to the conduction band is possible (Figure 9.11d).

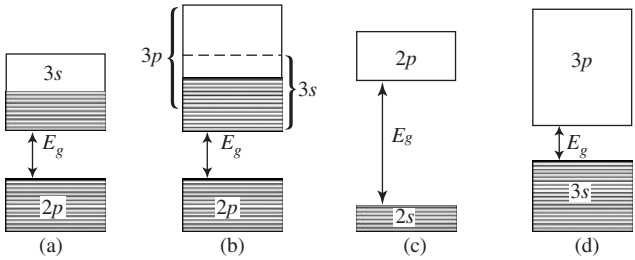

Figure 9.11 Band structure of different crystal types: (a) and (b) conductors, (c) dielectric, (d) semiconductors.

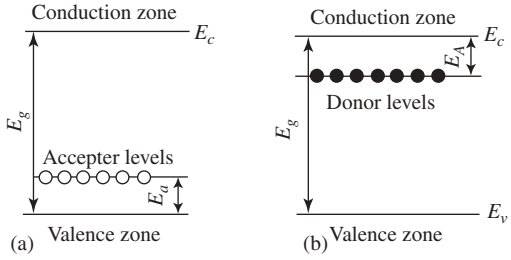

Figure 9.12 A band structure of doped semiconductors: (a) n-type, (b) p-type.

9.3 LATTICE DYNAMICS AND HEAT CAPACITY OF CRYSTALS

9.3.1 The Born–Karman model and dispersion curves

By crystal dynamics one usually understands the theory describing atomic oscillations around their equilibrium positions and those features of the properties that depend on these oscillations. Only harmonious oscillations occurring because of the action of quasi-elastic forces will be considered here (refer to Chapters 2.2 and 2.4).

Being independent, oscillations of all atoms can be described by a system of running waves with certain frequencies, polarization and wave vectors (see Section 2.9.5). According to the general principles of particle-wave duality (refer to Chapter 7.1), each wave associates with a particle called a phonon with energy $\hbar\omega_S$, polarization s ($s = 1, 2, 3$) and momentum $\mathbf{p} = \hbar\mathbf{k}$. Since phonons exist only within a crystal they are related to the category of quasi-particles. Nevertheless, interaction of phonons with other particles (electrons, neutrons, etc.) occurs according to classical laws of collision (refer to Section 1.4.5).

Consider the simplest model of a crystal as a one-dimensional chain of identical atoms. Direct the chain along an axis x. Denote a period along the chain by the letter a, and let l be the number of the atom counted from an arbitrary chosen atom (Figure 9.13). Value x_l represents instant coordinate of atom l. In this model one more simplification is entered, namely, the nearest neighboring atoms are considered to be interacting among themselves only. Such a model is called the *Born–Karman* model. The equation of movement (Newton's second law) can be written for the atom l as

$$m\ddot{\xi}_l = -\beta[(\xi_l - \xi_{l-1}) - (\xi_{l+1} - \xi_l)] = -2\beta\left[\xi_l - \frac{\xi_{l+1} + \xi_{l-1}}{2}\right], \tag{9.3.1}$$

where β is a force constant and the expression in square brackets is the shift of the atom l from its equilibrium position. This system of equations can be solved, the solution being sought in the form of a running wave

$$\xi_l = \xi_0 \exp[i(\omega t + kla)]. \tag{9.3.2}$$

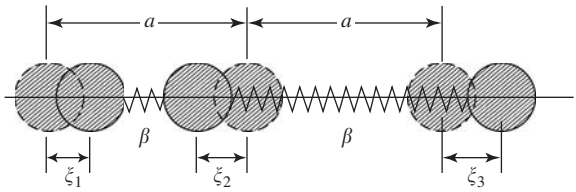

Figure 9.13 A one-dimensional chain of similar atoms with inter-atomic distance a (ξ is atom's deviation from the equilibrium position), β is a force constant of the inter-atomic bonds.

The connection between ω and k is

$$-\omega^2 m = \beta(\mathrm{e}^{\mathrm{i}ka} + \mathrm{e}^{-\mathrm{i}ka} - 2) = \beta(\mathrm{e}^{(\mathrm{i}ka/2)} + \mathrm{e}^{(\mathrm{i}ka/2)})^2 = -4\beta \sin^2 \frac{ka}{2}, \tag{9.3.3}$$

wherefrom

$$\omega = \sqrt{\frac{4\beta}{m}} \sin \frac{ka}{2}. \tag{9.3.4}$$

A *dispersion curve* is a curve of allowed ω-values as a function of k. Within the framework of the Born–Karman model this dependence is represented by eq. (9.3.4) (Figure 9.14). Let us look at its main points. Firstly, this equation is nonlinear; the dispersion of waves (refer to Section 2.9.4) is taking place. Secondly, this dependence is periodic; in space of wave vectors an independent (repeating) part is lasting from zero to π/a. This area is referred to as the *Brillouin zone* and a value π/a is the border (in this case –- one-dimensional border) of this zone: outside this zone the function $\omega(k)$ repeats periodically. Besides, the number of waves with various wavelengths is limited: from below by the period of a chain a, from above by the length of all chain L.

At small $k((ka / 2) \ll 1)$ $\sin(ka/2)$ in eq. (9.3.4) can be substituted by its argument. Then

$$\omega = \sqrt{\frac{\beta}{m}} ka \tag{9.3.5}$$

and the dependence $\omega(k)$ is getting linear. The wave phase speed can be derived from eq. (9.3.5) (refer to eq. (2.8.12)); this is an acoustic dispersion wave curve. The derivative $(d\omega / dk)$ is zero at the zone boundary. The dispersion curve is referred to as an acoustic branch.

A more complex model is a diatomic chain consisting of alternating atoms of different masses m_1 and m_2 which are located at equal distances from each other (which still equal a) and between which the same elastic forces operate (Figure 9.15). "The unit cell" of such a "crystal" is twice as large as the previous one. Two equations for movement should be written and solved together. The solution in the form of running

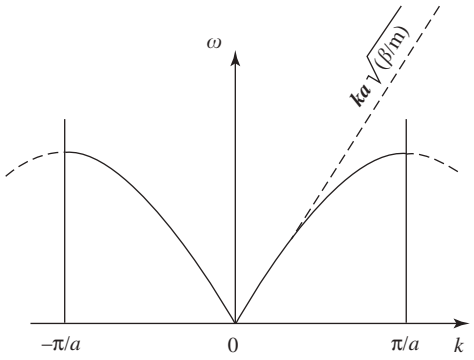

Figure 9.14 Dispersion curve $\omega(k)$ for Borman–Karman model.

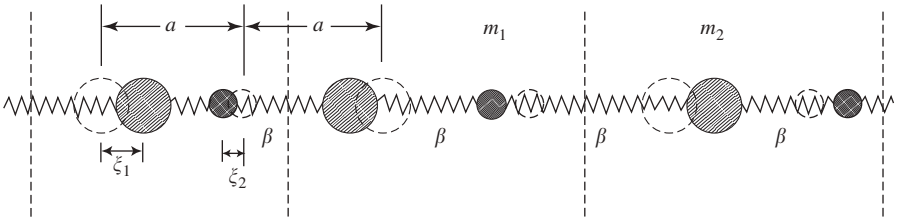

Figure 9.15 A one-dimensional model consisted of two different atoms with the same inter-atomic distance. A period is equal to 2*a*.

waves has the same appearance, but frequency ω depends on two masses and has two solutions:

$$\omega_{\pm}^2 = \beta\left(\frac{1}{m_1}+\frac{1}{m_2}\right) \pm \beta\sqrt{\left(\frac{m_1+m_2}{m_1 m_2}\right)^2 - 4\frac{\sin^2 ka}{m_1 m_2}}. \tag{9.3.6}$$

Accordingly, a graphic representation of the ω (k) function has two branches (Figure 9.16).

It is typical that one solution (ω_+) behaves in the same way as in the previous case. However another solution (ω_-) essentially differs: firstly, at $k \to 0$ frequency aspires to a nonzero value, secondly, at $k \to (\pi / 2a)$ the curve comes to different point on the Brillouin zone border. (The factor 2 in the denominator appeared because the identity period in the model presented in Figure 9.15 has changed.) The difference between frequencies on the Brillouin zone border is proportional to the distinction of masses of the two kinds of atoms. This second branch is referred to as an *optical branch*.

In a real three-dimensional crystal there are similar waves extending in all directions. Taking into account that in the crystal the existence of waves of three polarizations is possible (one being longitudinal L and two transverse wave T_1 and T_2, refer to Section 2.8.2),

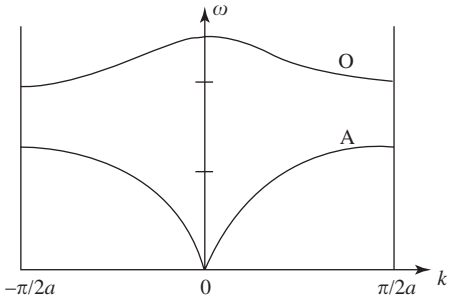

Figure 9.16 Graphical representation of dispersion curves $\omega(k)$ for the two-atomic chains. Acoustic (A) and optic (O) branches are presented.

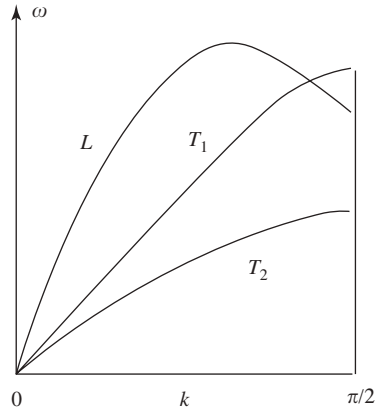

Figure 9.17 A general case of dispersion curves of three different kinds: L—longitudinal wave, T—two transverse waves.

three branches $\omega(k)$ can occur (Figure 9.17). In some crystals their degeneration is probable: two or all three branches can merge into one.

Similarly to the one-dimensional chain, the borders within the framework of which function $\omega(k)$ is independent are outlined. Such borders form the three-dimensional Brillouin zone. The picture of the dispersion curves dependent on direction and from wave polarization, becomes complex and, frequently, confusing. Figure 9.18 shows an example of experimentally measured dispersion curves in an aluminum crystal for the different directions specified in the figure; Figure 9.19 presents an example of the oscillation frequency distribution function $g(\omega)$.

Note that the acoustic branch corresponds to the oscillation of the crystal unit cells relative to each other, whereas the optical branches describe the oscillation of atoms relative to each other within the volume of a single unit cell.

Since the elastic waves in crystals are caused by atomic oscillations and are interconnected, waves are developed as *collective excitations*. Hence, in modern terminology,

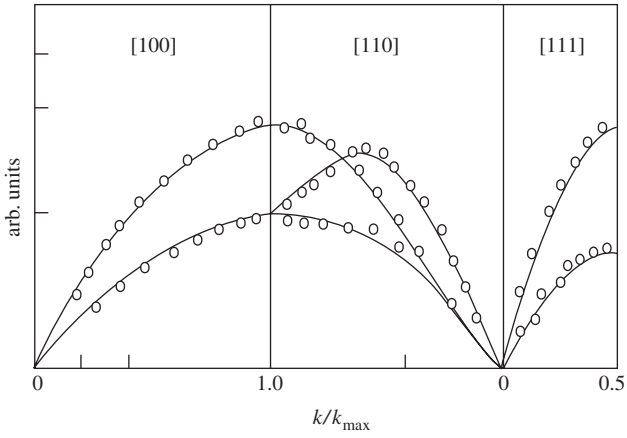

Figure 9.18 Dispersion curves for different crystallographic directions (shown in the scheme) in aluminum obtained by the neutron inelastic scattering method.

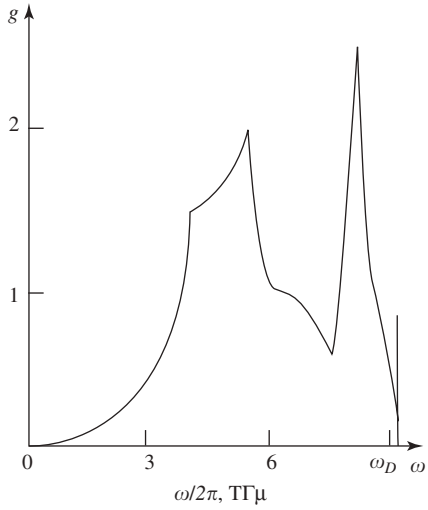

Figure 9.19 The experimental frequency density distribution $g(\omega)$ for aluminum (ω_D is the Debye frequency).

lattice heat capacity is a development of collective excitation in solids, i.e., the heat energy goes to phonon excitation (see below).

Participation of electron excitations in heat capacity is limited by quantum statistics laws (refer to Section 9.2.2). As only a small part of the electrons takes part in excitation, the electronic heat capacity usually makes a very small addition in comparison with the lattice one.

In a polycrystalline sample consisting of a large number of microcrystals, ideally—randomly dispersed in space—the resulting picture is averaged. As a result, the function $g(\omega)$, presents the projection of all dispersion branches to the axis of frequencies (phonon spectrum). It describes the distribution of oscillations on frequencies: product $g(\omega)d\omega$ gives the number of oscillations dz falling on an interval $d\omega$. In Figure 9.19 the experimentally measured function $g(\omega)$ for aluminum is given as an example.

The fluctuation distribution function determines the internal energy of a crystal:

$$U = \int \bar{\varepsilon} g(\omega) d\omega, \tag{9.3.7}$$

where $\bar{\varepsilon}$ is an averaged oscillation energy.

The dispersion curves and $g(\omega)$ function can be obtained by neutron scattering methods.

9.3.2 The heat capacity of crystals

Heat capacity was introduced in Section 3.4.3 as the heat energy capable of heating a body by 1 grad. For an ideal gas in molecular kinetic theory the mole heat capacity appeared to be equal to

$$C_V = \frac{i_{ef}}{2} R \text{ and } C_P = \frac{i_{ef}+2}{2} R,$$

where i_{ef} is the effective number of a gas molecule's degrees of freedom. In this case i_{ef} turns out to be the sum of translational, rotational and oscillation movements; in the latter $i_{ef,\,osc} = 2$ because oscillation simultaneously possesses potential and kinetic energy.

Apply these representations to a solid. For this purpose we should first analyze the character of possible movements of the molecules in it. Clearly, translational motion is excluded in this case. The rotation of molecules in a crystal is basically possible. For example, in crystal NH_4Cl a group NH_4^+ at different temperatures can make rotations around axes of different symmetry and sometimes exhibit a free rotation. However, the contribution of rotation to the thermal capacity of solids is appreciably less than oscillatory degrees of freedom. As a result only oscillations of atoms basically define the crystal thermal capacity. Furthermore, the three-dimensional character of a crystal should be taken into account.

The molar internal energy of a crystal U will then be given as a product

$$U = 3\frac{i_{ef,osc}}{2} RT = 3RT. \tag{9.3.8}$$

The derivative from internal energy on temperature gives a mole thermal crystal heat capacity C. As the volume of a crystal does not vary appreciably with temperature, we exclude index V. We shall then obtain

$$C = 3R, \tag{9.3.9}$$

i.e., the molar heat capacity of a crystal does not depend on temperature and is numerically equal to $3R$ ($\approx$ 25 J/(mol K)). This result is referred to as the Dulong–Petit law. Experiment shows that at moderate temperatures this law is carried out well enough for crystals with rather simple structure (Na, Al, Fe, Cu, Sn, etc.). However, crystals with more complex structures fail the Dulong–Petit law. So the atomic thermal capacity of a boron crystal is 14.2 and diamond is 5.7 J/(mol K). It has also been experimentally established that in the region of low temperatures the heat capacity falls as T^3, coming nearer to zero at $T \to 0$ K. The experimental facts therefore show that the simple classical theory considered is applicable only in a narrow temperature interval and for crystals with a simple structure.

The first quantum theory of heat capacity was suggested by Einstein. Einstein's model assumed that each atom in a crystal is an *independent* quantum oscillator (refer to Section 7.8.1). The energy spectrum of such an oscillator is presented in Figure 7.32. Because of the selection rule, the spectrum of absorption/emission contains only one frequency. A level's population is defined by the Boltzmann factor $\omega_E \sim \exp(E/\kappa T)$, i.e., the population gets less when the energy increases. In Section 6.6.3 it was shown that the average oscillator's energy is $\bar{\varepsilon} = (\hbar\,\omega) / (\exp\,(\hbar\,\omega / \kappa T) - 1)$ (eq. (6.6.13)). Accordingly, the internal energy U of one mole of a substance is

$$U = \omega_E \bar{\varepsilon} N_A = N_A \frac{\hbar\omega}{\exp(\hbar\omega/\kappa T) - 1} + U_0, \tag{9.3.10}$$

where U_0 is the zero oscillation energy. The latter is of no significance in the heat capacity of crystals.

The heat capacity C is obtained as

$$C = \frac{dU}{dT} = N_A \left(\frac{\hbar\omega}{\kappa T}\right)^2 \frac{\exp(\hbar\omega/\kappa T)}{(\exp(\hbar\omega/\kappa T) - 1)^2}. \tag{9.3.11}$$

Denoting the ratio $(\hbar\omega/\kappa)$ by θ, the last expression can be rewritten as

$$C = R\left(\frac{\theta}{T}\right)^2 \frac{\exp(\theta/T)}{(\exp(\theta/T) - 1)^2}. \tag{9.3.12}$$

The value θ is called the *characteristic temperature.* If one derives a function of the heat capacity upon T/θ for a series of simple substances, it will be represented by a single curve (Figure 9.20). It appears that Einstein's characteristic temperature θ defines the border behind which an essential deviation from the Dulong–Petit law takes place for every element. If we substitute the frequency $\omega = \sqrt{\beta\,/\mathrm{m}}$ (see eq. (2.4.5)) into the expression for the θ value, we can arrive at

$$\theta = \frac{\hbar}{\kappa}\sqrt{\frac{\beta}{m}}, \tag{9.3.13}$$

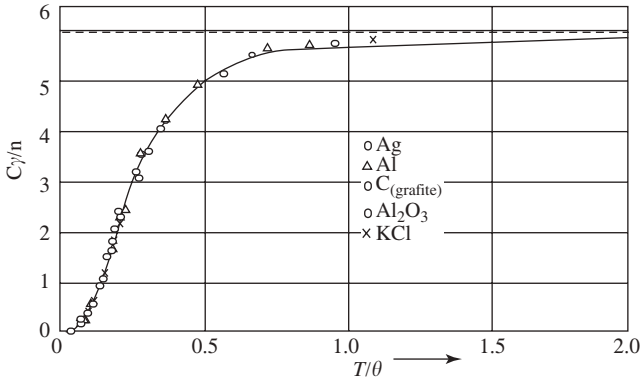

Figure 9.20 A reduced temperature dependence of heat capacity for some simple substances.

i.e., the θ value is inversely proportional to the square root from atomics' mass.

Let us consider some extreme cases. At $T \gg \theta$ the exponent can be decomposed into a series ($e^x \approx 1+x+\cdots$), and we can limit ourselves to the first two terms. For a system of one-dimensional oscillators we can arrive at

$$C \cong R\left(\frac{\theta}{T}\right)^2 \frac{1+(\theta/T)}{(\theta^2/T^2)} = R\left(1+\frac{\theta}{T}\right) \approx R$$

or for a three-dimensional crystal $C = 3R$, i.e., the Dulong–Petit law.

At $T \ll \theta$ the exponent in eq. (9.3.12) is much larger than 1. It gives $C \cong 3R\,(\theta\,/\,T)^2\, e^{-(\theta\,/\,T)}$, i.e., heat capacity is decreases with the decrease in temperature (because the exponent influence dominates over the term $(\theta\,/\,T)^2$).

Apparently, Einstein's model gives good conformity with Dulong–Petit at high temperature and explains the decrease of thermal capacity at low temperatures. However, it contradicts the law of approaching absolute zero: according to experiment, the corresponding curve should look like a cubic parabola T^3, whereas according to Einstein this dependence is described by the law $e^{-(1/T)}$.

P. Debye modified the Einstein's model by introduction of inter-atomic forces in a crystal model. This is equivalent as to take phonons into account (refer to Section 9.3.1). To each elastic wave (phonon) the Born-Karman atomic chain was attracted spread out in a three-dimensional array (Figure 9.13 and 9.15). As a result of reflection from external crystal borders, standing waves with various values ω and k (refer to Section 2.9.2 and 2.9.3) are formed. There is the certain relationship between the wavelength of standing waves λ and the size of the crystal L expressed by the eqn (2.9.8). Phase speed of running elastic wave υ_{Ph} is related to ω and k by expression (2.8.3) $\upsilon_{Ph}=\frac{\omega}{k}$, therefore

$$\omega = k\upsilon_{Ph} = \frac{2\pi\upsilon_{Ph}}{\lambda} = \frac{T\upsilon_{Ph}}{L}n, \tag{9.3.14}$$

where n is the number of the harmonic wave.

At the crystal volume V a large but limited number of standing waves are formed. The wavelengths of these standing waves are limited by the period of the crystal lattice from the short wavelength size ($\lambda > a$) and by the crystallite size L ($\lambda < L$) from the large one. Accordingly,

$$\omega_{\min} = \frac{2\pi v_{\text{ph}}}{\lambda_{\max}} = \frac{2\pi v_{\text{ph}}}{2L} = \frac{\pi v_{\text{ph}}}{L} \infty \tag{9.3.15}$$

and

$$\omega_{\max} = \frac{2\pi v_{\text{ph}}}{\lambda_{\min}} = \frac{\pi v_{\text{ph}}}{a}. \tag{9.3.16}$$

These values limit the range of frequencies. The number of standing waves dz is proportional to the elementary volume $4\pi\omega^2 d\omega$.

For a cubic crystal with volume $V = L^3$ the number of harmonics (normal oscillations) in the limits from 0 to ω is equal to $z = (2L/\lambda_n)^3 = 8\,(V/\lambda_n^3)$ or more precisely

$$z = \frac{4\pi V}{\lambda_n^3} = \frac{V}{2\pi^2 v_{\text{ph}}^3}\omega^2. \tag{9.3.17}$$

Differentiating z by ω we can obtain the frequency distribution $g(\omega)$ as

$$g(\omega) = \frac{dz}{d\omega} = \frac{3V}{2\pi^2 v_{\text{ph}}^3}\omega^2. \tag{9.3.18}$$

The Debye function $g(\omega)$ is depicted in Figure 9.21.

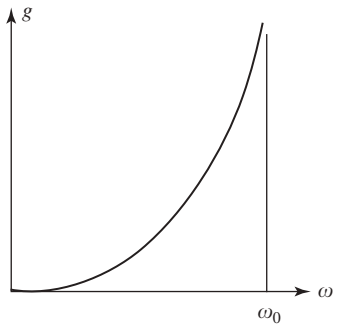

Figure 9.21 The frequency density distribution $g(\omega)$ in the framework of the Debye model (ω_{D} is the Debye frequency).

The maximum spectrum frequency is called the Debye *characteristic frequency* ω_D. It can be determined from the normalization to the total number of normal frequencies (the number of standing waves).

$$\int_0^{\omega_D} g(\omega)d\omega = \frac{V\omega_D^3}{2\pi^2 v_{ph}^3} = 3N,$$

from which

$$\omega_D = v_{ph}\left(\frac{6\pi N}{V}\right)^{1/3}.$$

The notion of "characteristic temperature" acquires a new meaning:

$$\theta = \frac{\hbar\omega_D}{\kappa T}. \tag{9.3.19}$$

According to eq. (9.3.7) the general expression for U in a given case is:

$$U = \int_0^{\omega_D} \overline{\varepsilon} g(\omega)d\omega = \int_0^{\omega_D} \frac{\hbar\omega}{\exp(\hbar\omega/\kappa T - 1)} \times \frac{9N}{\omega_{max}^3}\omega^3 d\omega. \tag{9.3.20}$$

Differentiating over temperature, we can obtain the crystal heat capacity

$$C = \frac{dU}{dT} = 3R\left[12\left(\frac{T}{\theta}\right)^3 \int_0^{\theta/T}\left(\frac{x^3 dx}{e^x - 1} - \frac{3(\theta/T)}{e^x(\theta/T) - 1}\right)dx\right]. \tag{9.3.21}$$

The expression in square brackets is the *Debye function.* This function is tabulated. We shall find extreme values of heat capacity: at $T \gg \theta_D$ the Debye function aspires to 1 and $C \to 3R$; at $T \ll \theta_D$ the integral in the Debye function is close to 1 and $C \to (T/\theta)^3$. Good consent with experiment is achieved.

Figure 9.22 shows the results of comparative approaches for three models of crystal dynamic properties.

In conclusion, we give in Table 9.2, the Debye temperature for some substances.

Despite the success of the theory, it is necessary to ascertain whether its use in practice meets many difficulties. This is visible even from a comparison of the curves of dependence $\omega(k)$, obtained theoretically and experimentally (with the help of inelastic scattering of thermal neutrons) (Figures 9.19 and 9.21). At concurrence of some features of the curves (square dependence at small phonon wave vectors k, sharp decrease at certain values of frequencies, etc.) a definite difference can also be found. The theory allows one to

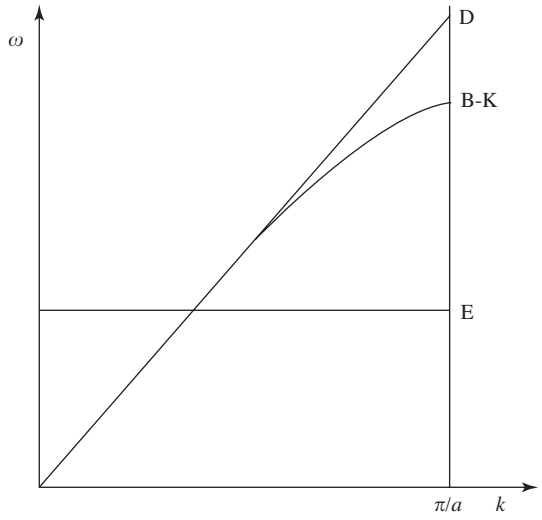

Figure 9.22 Comparison of the $g(\omega)$ function for different models: Born–Karman (B–K), Einstein (E) and Debye (D).

Table 9.2

Debye temperature values for some simple substances

Substance	Debye temperature (K)
C (diamond)	1910
Be	1160
Si	658
Cr	420
Pb	95

obtain only estimated or comparative values of heat capacity; therefore experimental data are often used in serious work.

A promising direction in chemical technology developments in the last 10 years is nanotechnology, i.e., the syntheses of materials consisting of microscopically small particles (clusters), small in number ($N \sim 10^3$ atoms), being comprised on the "nanoscale" $L \sim 10^{-9}$ m. This technology gives us a good assurance that this chapter is of use in the book. In practice, this border is somehow degraded, because in technology by "nanoparticle" one usually implies an atomic or molecular object, the internal energy of which complies in order of magnitude with its surface energy. More important is the fact that the mechanical, electrical, magnetic and other characteristics of nanoparticles are vastly distinct from similar characteristics of the same bulk material. Some of thesxe characteristics are directly connected with the nanoparticle's size, so this opens the way to adjust them to a goal-directed image. This fact permits one to produce new materials with predetermined properties, e.g., semiconductors that are required for creating more reliable generations of computers.

Let us consider as an example the well-known Debye theory of the heat capacity of crystals. The internal energy of a bulk crystal minus zero energy is given in this theory by an equation

$$U_\infty = \frac{9N\kappa T^4}{\theta_D^3} \int_0^{\frac{\theta_D}{T}} \frac{x^3}{e^x - 1} dx,$$

where $x = (\hbar\omega / \kappa T)$

A nanoparticle is distinguished from a bulk crystal since its phonon spectrum is truncated not only from the site of high frequencies but from low frequencies as well (refer to Example E9.5).

Let us consider the averaged solid nanoparticle model with number of atoms N, crystal lattice period a, primitive cubic lattice with the unit cell volume V and linear size L.

The physicochemical features, however, and in particular the nanoparticle's heat capacity in the implicit description can depend on their forms, for instance, by the way it fastens to the substrate and the nature of interaction with it, i.e., from border conditions. A detailed consideration of all these factors forms the subject for specialized future studies. Therefore, the further evaluations are based on the assumption of the independence of the nanoparticle's thermal characteristics from the particular type of border conditions (similar to that of the classical theories of Einstein and Debye).

The longest wavelength λ corresponds to the lowest frequency of the nanoparticle that can be put in correspondence to the temperature, i.e.,

$$\theta_N = \frac{\hbar\omega_N}{\kappa} = \frac{2\pi\hbar\upsilon}{\lambda_N\kappa},$$

therefore,

$$\theta_N = \frac{2\pi\hbar\upsilon}{2N^{1/3}a\kappa} = \frac{\pi\hbar\upsilon}{N^{1/3}a\kappa} \approx \frac{\pi\hbar\upsilon}{L\kappa}.$$

Since the Debye temperature is assumed to be $\theta_D = (\pi\hbar\upsilon / a\kappa)$, the ratio $(\theta_N/\theta_D) = N^{-1/3}$ or $(\theta_N / \theta_D) \approx 1/10$ with $N \approx 10^3$. Therefore, nanoparticles have two characteristic temperatures that distinguish them from that of the bulk materials: the usual Debye temperature θ_D and the temperature θ_N both depend on the particle size.

For further simplification, let us restrict ourselves to the limit that corresponds to the condition $\theta_D > T$, because of the fact that this condition corresponds to the lowest value of $x = (\hbar\omega / \kappa T) = (\theta_N T) > 1$. This permits us to simplify the integral expression, i.e., assume $e^x \gg 1$. In this case the internal energy of the nanoparticle in the low temperature approximation is equal to

$$U_N = \frac{9N\kappa T^4}{\theta_D^3} \int_{\frac{\theta_N}{T}}^{\infty} x^3 e^{-x} dx = -\frac{9N\kappa T^4}{\theta_D^3} (x^3 + 3x^2 + 6x + 6) \Big|_{\frac{\theta_N}{T}}^{\infty}$$

For diamond dust (θ_D = 2230 K), $L \sim 10a$, $N \sim 10^3$, $\theta_N = (\theta_D/10) \sim 223$ K, i.e., the condition $(\theta_N / T) > 2$ is fulfilled at temperatures $T < 111$ K. At $e^x \gg 1$ the expression for the nanoparticle heat capacity is changed as well. The Debye equation at $T \ll \theta_D$, i.e.,

$$C = 9Nk\left(\frac{T}{\theta_D}\right)^3 \int_0^{\infty} \frac{x^4 e^x dx}{(e^x - 1)^2}$$

can be simplified by decomposition to

$$C_N = 9Nk\left(\frac{T}{\theta_D}\right)^3 \int_{\frac{\theta_N}{T}}^{\infty} x^4 e^{-x} dx = -9Nk\left(\frac{T}{\theta_D}\right)^3 (x^4 + 4x^3 + 12x^2 + 24x + 24)e^{-x} \Bigg|_{\frac{\theta_N}{T}}^{\infty}.$$

The well-known classical Debye law for bulk crystals $C_\infty \sim \alpha T^3$ is disobeyed, and, as the calculations show, rather significantly. Once more, this confirms the fact that nanoparticles really are new materials, with physicochemical characteristics greatly different from the characteristics of materials with the same chemical composition but in the bulk state.

EXAMPLE E9.4

Determine the amount of heat ΔQ for NaCl of mass m = 20 g heated at ΔT = 2 K in two cases (1) from $T_1 = \theta_D$ and (2) T_2 = 2 K. Accept the characteristic Debye temperature θ_D to be equal to 320 K.

Solution: In general, the amount of heat ΔQ needed to heat a system from τ_1 to τ_2 can be calculated according to the expression $\Delta Q = \int_{\tau_1}^{\tau_2} C dT$ where C is the heat capacity of the system. The heat capacity of a body is related to molar heat capacity $C = (m/M)C_m$ where m is body mass and M is molar mass(refer to Section 3.4.3). Substituting into the integral gives $\Delta Q = \frac{m}{M} \int_{\tau_1}^{\tau_2} C_M d T$ *. In a general case, C_M depends on T and therefore it is not allowed to take it out of the integral sign. However, in the first case we can neglect the C_M change and consider it to be constant, throughout the interval ΔT, equal to $C_M(T_1)$. Therefore, the integral takes the form $\Delta Q = (m/M)C_M(T_1)\Delta T$**. The molar heat capacity in Debye theory is given by eq. (9.3.21). In the first case calculations give C_M = 2.87 R. Substituting this result into ** we obtain $\Delta Q = 2.87(m/M)R\Delta T$ and executing calculations we arrive at ΔQ = 16.3 J.

In the second case ($T \ll \theta_D$) calculation of ΔQ is simplified by the fact that we can use the limited property of the Debye law where the heat capacity is

proportional to T^3: we cannot use the previous approximation but have a mathematical expression for

$$C_{\mathrm{M}} = \frac{12\pi^4}{5} R \left(\frac{T}{\theta_{\mathrm{D}}} \right)^3 .$$

$$\Delta Q = \frac{12\pi^4}{5} \frac{m}{M} \frac{R}{\theta_{\mathrm{D}}^3} \int_{T_2}^{T_2+\Delta T} T^3 dT.$$

Executing integration we obtain

$$\Delta Q = \frac{12\pi^4}{5} \frac{m}{M} \frac{R}{\theta_{\mathrm{D}}^3} \left[\frac{(T_2 + \Delta T)^4}{4} - \frac{T_2^4}{4} \right].$$

Since $T_2 + \Delta T = 2T_2$ this equation takes the form

$$\Delta Q = \frac{3\pi^4}{5} \frac{m}{M} \frac{R}{\theta_{\mathrm{D}}^3} 15 T_2^4 \text{ or } 9\pi^4 \frac{m}{M} \frac{R}{\theta_{\mathrm{D}}^3} T_2^4 .$$

Substituting all known values and executing calculations we obtain $\Delta Q = 1.22$ mJ.

EXAMPLE E9.5

How much does the amount of heat required differ for heating a nanoparticle consisting of N atoms from temperature $T_1 = 0$ K to $T_2 = \theta_{\mathrm{D}}/50$, compared to the amount of heat required to heat the same amount of particles in the form of a bulk crystal. Accept the nanoparticle's size $L = 10a$, a being the period of the crystal lattice; θ_{D} is the Debye temperature).

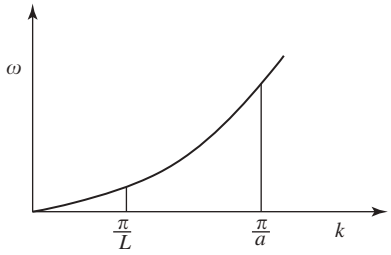

Solution: The frequency of a nanoparticle's dependence on the wavenumber k is depicted in the Figure E9.5. From the problem's conditions, we have

$$\frac{\theta_{\mathrm{D}}}{\theta_{\mathrm{N}}} = \frac{\alpha}{L} = \frac{1}{10}.$$

The internal energy U of a bulk crystal consisting of N atoms at $T_1 = T_2$ is equal to

$$U_{\mathrm{N}} = \frac{9N\kappa T^4}{\theta_{\mathrm{D}}^3} \int_0^{\frac{\theta_{\mathrm{D}}}{T_2}} \frac{x^3 dx}{\mathrm{e}^x - 1}.$$

The upper limit in the task is $(\theta_{\mathrm{D}} / T_2) = 50 \gg 1$, therefore one can accept it, as usual, to be equal to ∞. The tabular point

$$\frac{\theta_{\mathrm{D}}}{T_2} = 50 \gg 1, \quad \int_0^{\infty} \frac{x^3}{\mathrm{e}^x - 1} = \frac{\pi}{15} = 6.5.$$

For $T = T_2$ the internal energy is

$$U_{\mathrm{N}} = \frac{9N\kappa T_2^4}{\theta_{\mathrm{D}}^3} \int_{\frac{\theta_{\mathrm{N}}}{T_2}}^{\infty} x^3 \mathrm{e}^{-x} dx,$$

where

$$\frac{\theta_{\mathrm{N}}}{T_2} = \frac{50}{10} = 5.$$

The zero energy as independent of temperature cannot be taken into account. The integral in the last expression for U_{N} can be calculated in parts:

$$\int_5^{\infty} x^3 \mathrm{e}^{-x} dx = -(x^3 + 3x^2 + 6x + 6)\mathrm{e}^{-x} \Big|_5^{\infty} = 1.57$$

Then the ratio $(U_{\infty}) / (U_{\mathrm{N}}) = (6.5 / 1.57) \approx 4.15$, i.e., the internal energy difference for a bulk crystal and a nanoparticle with equal amounts of atoms is really very significant.

EXAMPLE E9.6

Using a free electron model calculate for potassium at 0 K: (1) Fermi energy ε_F, (2) Fermi temperature T_F, (3) the ratio of averaged potential energy $\langle U\rangle$ of the two adjacent electrons in the electron gas to their averaged kinetic energy $\langle\varepsilon\rangle$. Assume the potassium density $\rho = 860$ kg/m^3 and atomic mass $A = 39.1 \times 10^{-3}$ kg/mol.

Solution. Although in general in the main text we can come to the conclusion that the free-electron model is applicable to crystals, we can use in some cases, with certain limitations, the classical approach to the evaluation of electron gas properties.

(1). At $T = 0$ K, the Fermi energy (refer to Section 9.2.2) depends only on the electron concentration n $\varepsilon_F = (\hbar^2 / 2m_e)(3\pi^2 n)^{2/3}$. Assume that every potassium atom gives one electron to the free electron gas state. Therefore, the concentration of free electrons is equal to the potassium atom concentration, namely $n = n_{at} = (\rho/A)N_A$. In order to avoid very large expressions and calculation we will deviate from our recommendation and calculate each quantity separately. Thus, we can calculate the electron concentration accordingly:

$$n = \frac{860}{39.1\times10^{-3}} 6.02\times10^{23}\ \mathrm{m}^{-3} = 1.32\times10^{28}\ \mathrm{m}^{-3}$$

We can calculate the Fermi energy according to the mentioned formula as

$$\varepsilon_F = \frac{(1.05\times10^{-34})^2}{2\cdot9.11\times10^{-31}}\left(3\pi^2\times1.32\times10^{28}\right)^{2/3}\mathrm{J} = 3.23\times10^{-19}\ \mathrm{J\ or\ 2.02\,eV}$$

(2) The Fermi temperature can be calculated from the equation $\varepsilon_F = \kappa T$: $T = \varepsilon_F/\kappa$. Executing calculations we obtain:

$$T_F = \frac{3.23\times10^{-19}}{1.38\times10^{-23}} = 2.34\times10^4\,\mathrm{K} = 23.4\ \mathrm{K}$$

(3) In order to find the zero temperature electron gas pressure we can use the expression $p = (2/3)\underline{n}\langle\varepsilon\rangle$. Here we will assume $\langle\varepsilon\rangle$ the averaged value of kinetic energy at $T = 0$ K. Find this expression using the distribution of the free electron upon energies $dn(\varepsilon) = (1/2\pi^2)(\hbar^2/2m_e)^{3/2}\,\varepsilon^{1/2}\,d\varepsilon$, where $dn\,(\varepsilon)$ is the number of electrons in a unit volume, the energy of which lie in the small interval from ε to $\varepsilon + d\varepsilon$. Then $dn(\varepsilon) = C\varepsilon^{1/2}d\varepsilon$, where C is a constant. We can find the averaged value $\langle\varepsilon\rangle$ for free electrons by dividing the total energy in an unit volume by their concentration, i.e.,

$$\langle\varepsilon\rangle = \frac{\int_0^{\varepsilon_F}\varepsilon dn}{\int_0^{\varepsilon_F} dn} = \frac{C\int_0^{\varepsilon_F}\varepsilon^{3/2}d\varepsilon}{C\int_0^{\varepsilon_F}\varepsilon^{1/2}d\varepsilon} = \frac{(2/5)\varepsilon_F{}^{5/2}}{(2/3)\varepsilon_F{}^{3/2}} = \frac{3}{5}\varepsilon_F$$

Substituting this result into the expression for free electron gas pressure $p = (2/3)\, n\, (3/5)\, \varepsilon_F$ we obtain $p = (2/5)1.32 \times 10^{28} \times 3.23 \times 10^{-19} = 1.71 \times 10^9$ Pa $= 1.68 \times 10^4$ atm.

(4) The averaged potential energy of the electrostatic interaction of two point charges (refer to eq. (4.1.21)) $\langle U \rangle = (e^2)/(4\pi\varepsilon_0 \langle l \rangle)$ where $\langle l \rangle$ is an averaged distance between two adjacent electrons of the degenerated electron gas (refer to Example E3.1) $\langle l \rangle = n^{(1/3)}$. Then $\langle U \rangle = (e^2 n^{1/3}) / (4\pi\varepsilon_0)$. We already know the $\langle \varepsilon \rangle$ (see above) therefore

$$\frac{\langle U \rangle}{\langle \varepsilon \rangle} = \frac{e^2 n^{1/3}}{4\pi\varepsilon_0} \frac{5}{3\varepsilon_F} = \frac{5e^2}{12\pi\varepsilon_0} \frac{n^{1/3}}{\varepsilon_F}.$$

Substituting the numerical values into this expression we arrive at

$$\frac{\langle U \rangle}{\langle \varepsilon \rangle} = \frac{5(1.6)^2}{12\pi \times 8.85 \times 10^{-12}} \frac{(1.32 \times 10^{28})^{1/3}}{3.23 \times 10^{-19}} = 2.81$$

9.4 CRYSTAL DEFECTS

A crystal represents a complex quantum mechanical system with an enormous amount of particles with a strong interaction between them. If all the particles are located in space strictly ordered with the formation of an ideal three-dimensional crystal structure, then such a system possesses minimal free energy. In a real crystal, however, the ideal periodicity is often broken due to inevitable thermal fluctuations: some atoms break periodic array, abandon their ideal position and produce a defect. The frequency and amount of fluctuations are defined by the Boltzmann factor, i.e., they depend on temperature and binding strength or, in other words, on the depth of the potential well corresponding to the regular position of atoms.

The role of defects in crystal properties is very high. On the other hand, new and improved old methods of defect crystal structure studies have appeared. This leads to the fact that, in recent decades, there has been extensive investigation into the physics of solids from the point of view of their deflection from perfection. Natural and new synthetic materials are being investigated.

Let us distinguish point (zero-dimensional) and extended defects (dislocations).

9.4.1 Point defects

Point defects can appear in a small area of the crystal, not exceeding several internuclear distances. Due to thermal fluctuations, a single atom can abandon its ideal position and occupy a position in the so-called interstitials (a position, though having a potential well, is of small depth). The regular position in the lattice remains empty, and is called a *vacancy.* Such pair defects are referred to as Frenkel's defects, they contain a vacancy in a regular array and interstitial atoms (Figure 9.23).

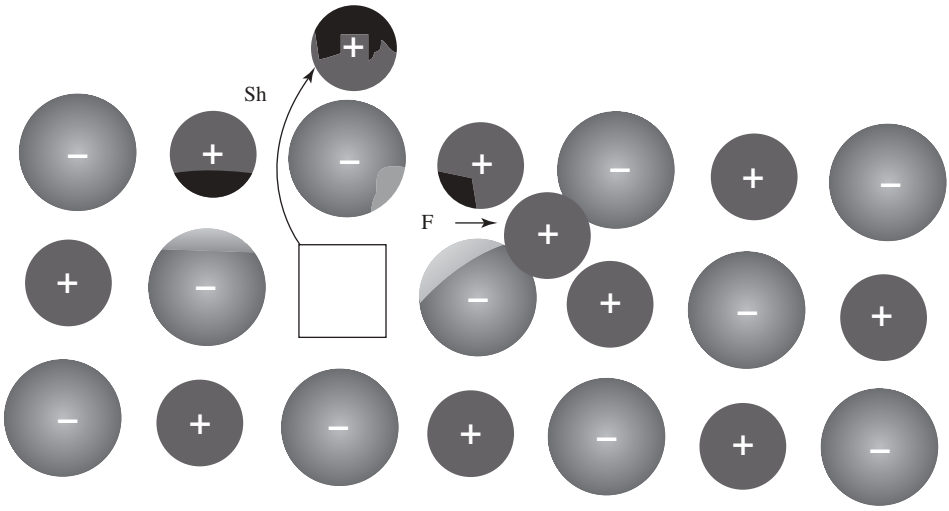

Figure 9.23 The Frenkel (F) and Schotky (Sh) types of point defect in a crystal.

If an atom comes out onto a crystal surface and leaves a vacancy in its regular position, then such a single defect is referred to as a Schotky defect.

The probability of a Schotky defect formation is proportional to the Boltzmann factor $P\sim \exp(-E_{\text{sh}}/\kappa T)$, where E_{sh} is the energy required for an atom's removal from its regular position to the crystal surface. If N is the total amount of atoms and n is the vacancy number then $P = n/(N-n) = \exp(-E_{\text{sh}}/\kappa T)$ or, at $n \ll N$,

$$\frac{n}{N} \approx \exp\left(\frac{-E_{\text{sh}}}{\kappa T}\right). \tag{9.4.1}$$

Estimations show that at $T \approx 1000$ K and vacancy activation energy $E \approx 1$ eV, the relative vacancy concentration is $(n/N) \approx e^{-12} \approx 10^{-5}$. Note that the relative vacancy concentration is proportional to $\exp(-1/T)$.

The number of Frenkel pair defects n depends on the number of regular positions in the crystal N and the number of interstitials N'

$$n \sim (N \times N')\exp\left(\frac{-E_{\text{F}}}{\kappa T}\right),$$

where E_{F} is the energy required for an atom's disposition from the regular site into the interstitial. The vacancies in ionic crystals are mostly Frenkel defects.

Crystal defects are not static. They wander around the crystal: a neighboring atom occupies the vacant position; the interstitial atom can occupy a regular site, etc. Only their relative number is determined by the Boltzmann factor.

Along with such elementary defects, more complex ones can also appear; for example, divacancy, the formation of which is energetically more favorable in comparison with two individual vacancies. Besides, the mobility of a divacancy is higher than that of individual vacancies. The congestion of many vacancies leads to the formation of the so-called clusters. Vacancies strongly influence diffusion and related processes.

Elastic displacements in the area surrounding a point defect decrease proportionally to $1/r^3$, where r is the distance from the defect. This shows that distortions in the neighborhood of a defect can be rather significant, but quickly falls down at distance.

Possessing mobility, the point defects can interact with each other and with other defects. On meeting, the vacancy and interstitial atom can annihilate each other.

An important role in vacancy formation is played by impurity atoms. They can replace regular atoms, and also be in interstitials. In particular, in the crystal structure KCl the replacement of K by Ca atoms leads to the occurrence of vacancies.

Small amounts of impurities considerably change the electric properties of semiconductor crystals.

9.4.2 Dislocations

Apart from point defects, there also exist extended, in particular, one-dimensional edge, dislocations: a failure of a crystal lattice having in one direction a long (even macroscopic) dimension but small sizes in the other directions (one or several internuclear distances). Such defects play a very important role in the formation of many properties of crystals, in particular, mechanical properties.

Quantitatively, the extended failure of the crystal lattice is described by the so-called Burgers vector. Let it be described in a simple cubic crystal. In Figure 9.24 a plane (001) of such a crystal is presented.

In an ideal nondeformed lattice we shall choose a closed contour and number the atoms included in this contour (Figure 9.24a). Such a contour is called *Burger's contour*. Travelling toward the east over the contour for two periods, south for two periods, then

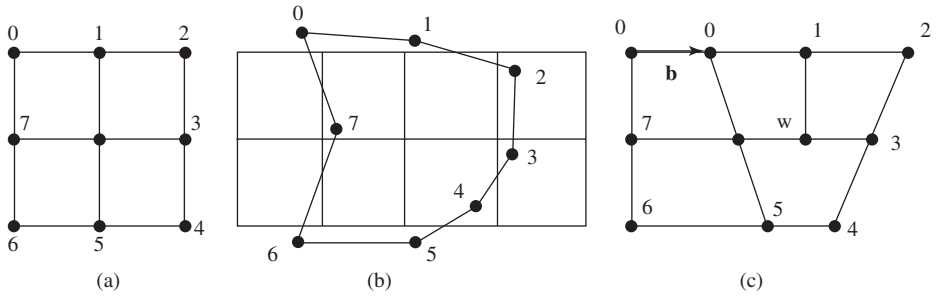

Figure 9.24 Burger's vector in (a) an ideal, (b) an elastically deformed and (c) a crystal with edge dislocation.

west and, finally north, we will arrive at the initial atom. In a numerical expression, the travel over the contour is 0–1–2–3–4–5–6–7–0. If a crystal is elastically deformed the atoms, being close to their ideal positions, are displaced by small distances (Figure 9.24b): the contour is deformed but still remains closed.

Now create a defect in the crystal as a half-plane (i.e., an infinite plane in two directions limited by a line in the third side) and introduce it into the crystal parallel to similar crystallographic planes (Figure 9.24c). Now, traveling over Burger's contour we will not come to the initial atom but to another point. To close the contour, it is necessary to draw a closing vector **b**, which is referred to as *Burger's vector.* Note that Burger's vector is perpendicular to the plane introduced.

Dislocation is a linear crystal defect for which Burger's vector is not zero. This definition is common for rather large numbers of a different kind of linear defect. The considered dislocation is referred to as an edge disposition; the extreme line (edge) of the induced plane is referred to as the *line of dislocation* (in Figure 9.24c this line in a point *w* is perpendicular to the plane of drawing). For such a dislocation, Burger's vector is perpendicular to the dislocation line.

A model of edge dislocation made of balls is presented in Figure 9.25. In Figure 9.26 a three-dimensional image of the edge disposition with Burger's vector perpendicular to the plane is shown. The crystal above the dislocation edge is stretched and in its lower part is compressed.

Now consider another kind of disposition, namely, a *screw disposition.* Let us imagine a pile of sheets of paper. Using a sharp knife, cut it from the center of the pile to its edge. Shift the free paper edges perpendicular to the sheets by the thickness of one sheet. Sticking the edges of the new planes to the edges of the old ones will result in a spiral. This spiral gives a graphic representation of screw dislocation. Its crystallographic image is given in Figure 9.27.

Dislocations can move in crystals as do point defects; the edge dislocation is presented in Figure 9.28. Under the action of an external pressure the shift of the upper part of the

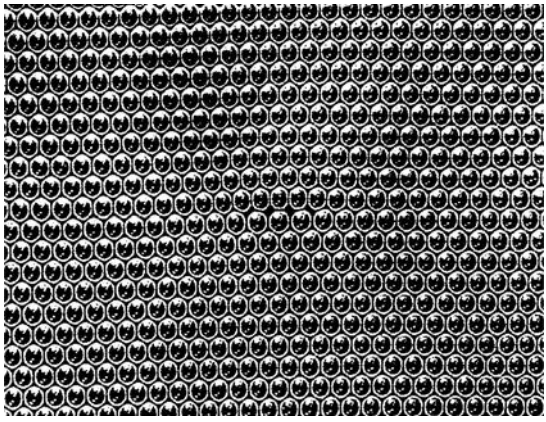

Figure 9.25 A ball model of the edge dislocation.

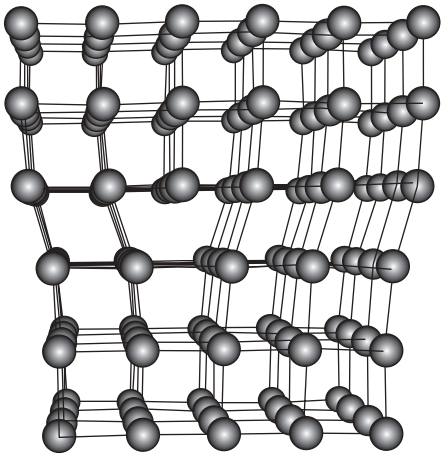

Figure 9.26 A three-dimensional image of the edge dislocation.

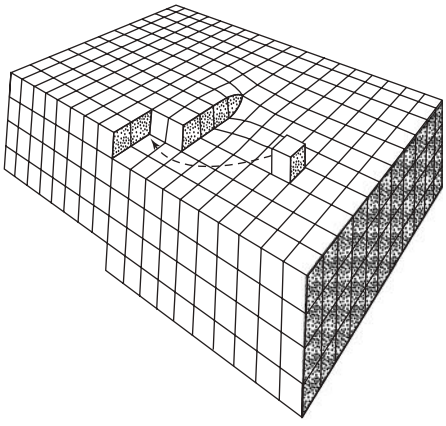

Figure 9.27 A model of a screw dislocation.

crystal has forced the dislocation to be switched to the next atomic plane and, finally, to appear on the crystal surface. Similar movements can make screw dislocation too.

There exist bigger crystal defects called *small-angle boundaries*. The scheme of such a boundary is depicted in Figure 9.29. It can be imaged by a set of number of edge dislocations.

The presence of imperfections essentially influences the mechanical properties of crystals. Experience shows that theoretically calculated strength properties appear, as a rule, to be appreciably higher than experimental ones; this is caused by neglecting crystal imperfections. Table 9.3 lists the physical methods that allow the investigation of the real structure of crystals.

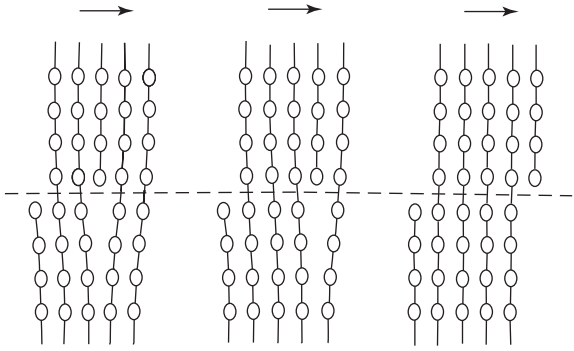

Figure 9.28 A scheme of an edge dislocation movement.

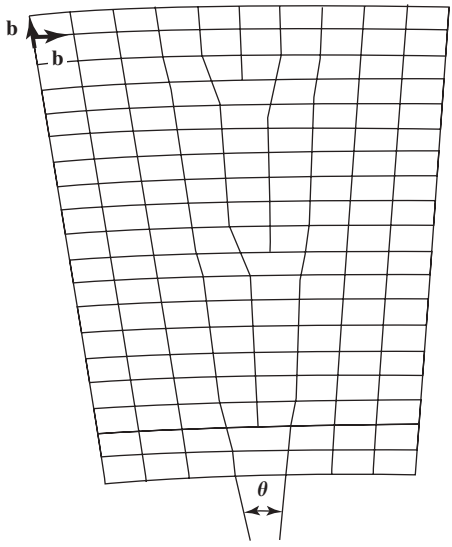

Figure 9.29 A low-angle edge.

Table 9.3

Methods of investigation of crystal defects

Method	Object thickness	Width of image	Maximal defects density (cm^2)
Electron microscopy	>100 nm	≈10 nm	$10^{11}-10^{12}$
X-rays' transmission	0.1−1.0 mm	5 μm	10^4-10^5
X-rays' reflection	<2/50 μm	0.5 μm	10^6-10^7
Metal sputtering onto surface[a]	≈10 μm	0.5 μm	$2\times\cdot 10^7$
Etching pits[b]	No limits	0.5 μm	4×10^8

[a]Sputtering of thin layers onto a surface and observation of dislocation by different methods.
[b]Surface etching and observation of etching pits by different methods.

9.5 TRANSPORT PHENOMENA IN LIQUIDS AND SOLIDS

The laws of transport phenomena in states other than gases differ among themselves in many respects. This distinction is defined mainly by the difference in their atomic structure. This will be explained using the example of a monoatomic crystal with a cubic structure (refer to Table 9.1).

The *function of radial distribution* $G(r)$ has great value in this respect. To explain the physical sense of this function, we shall define one more concept: the *coordination sphere*, perhaps known to readers from chemistry. For this purpose we choose in the crystal any atom and superpose it with the coordinate system origin. Allocate around it a spherical layer of radius r and thickness Δr ($\Delta r \ll r$); the layer volume is $\Delta V = 4\pi r^2 \Delta r$. The corresponding scheme is shown in Figure 9.30; for simplicity a two-dimensional section of a cubic lattice is used. If $r = r_1$ no atom falls onto the sphere. When r is less than the shortest interatomic distance a no atom falls into the spherical layer either. At $r = a$ all atoms which meet at this distance fall into the spherical layer (in a three-dimensional cubic crystal there are six such atoms). With a further increase of r in an interval $a < r < \sqrt{2}a$, again no atoms fall in the layer, but at $r = \sqrt{2}a$ atoms do fall again in the layer; their number in the three-dimensional array will be 12. At $r = \sqrt{3}a$ in the layer eight atoms will fall. This procedure can be continued further. These spheres are referred to as *coordination spheres* and the numbers of atoms falling onto them as *coordination numbers.*

Count the number of atoms ΔN enclosed in the spherical layer $4\pi r^2 \Delta r$. Write this number as:

$$\Delta N = 4\pi r^2 \, \Delta r \, n_0 G(r).$$

Here n_0 is the average over the whole crystal volume atomic concentration, and $G(r)$ is the radial distribution function. Wherefrom:

$$G(r) = \frac{\Delta N}{\Delta V n_0} = \frac{\Delta N}{4\pi r^2 \, \Delta r \, n_0} = \frac{n(r)}{n_0}, \tag{9.5.1}$$

where $n(r)$ is the local atomic concentration in the spherical layer with radius r.

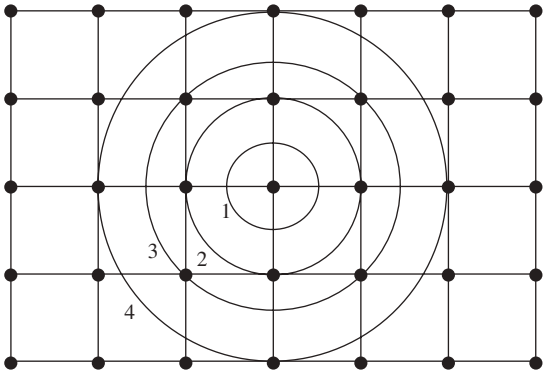

Figure 9.30 Coordination spheres in a crystal. A two-dimensional section of a cubic crystal is presented. Numbers denote the first, second, third and fourth coordination spheres.

It can be seen from the last expression that when the atomic concentration in the allocated spherical layer is equal to average concentration n_0, $G(r) = 1$. The function of radial distribution is distinct from unity only in the case when the concentration of atoms in the allocated layer is different from n_0. Hence $G(r)$ characterizes the concentration deviation in a specified layer from the average value.

The functions $G(r)$ for gases, liquids and crystals are presented in Figure 9.31. In crystals atoms are arranged in the ordered lattice; they are at certain distances from each other. The $G(r)$ function is different from zero when r is equal to one of the possible interatomic distances, i.e., when r touches the coordination sphere. In the resultant radial distribution function $G(r)$ in a crystal is represented by a system of discrete peaks (Figure 9.31a). The regular arrangement of peaks in crystalline solids specifies the presence in a crystal *of the long-range order*. If atoms are at rest in their ideal positions, function $G(r)$ is represented by a system of discrete, narrow spectral lines. Because of the thermal vibrations of atoms around their regular positions the lines are widened.

In gases $G(r) \equiv 1$; this means that there is a total disorder in gases. However, because gas atoms cannot approach each other closer than $r = d_{эф}$ in an area $r < d_{ef}$ function $G(r)$ falls to zero (Figure 9.31c). All this corresponds to an absence of even short-range order in gases; the full disorder in an arrangement of atoms.

It has been experimentally established that function $G(r)$ in liquids looks like that presented in Figure 9.31b: there are dim maxima at $r < (1 \div 3)\, a$, and further $G(r)$ aspires to 1. This result indicates some order in an arrangement of atoms in the liquids at specified distances and the absence of order at large r. Such a situation corresponds to *the short-range order.* It can be imagined as a presence in liquids of very small crystallites, completely disordered to each other. Due to the thermal motion of atoms these crystallites

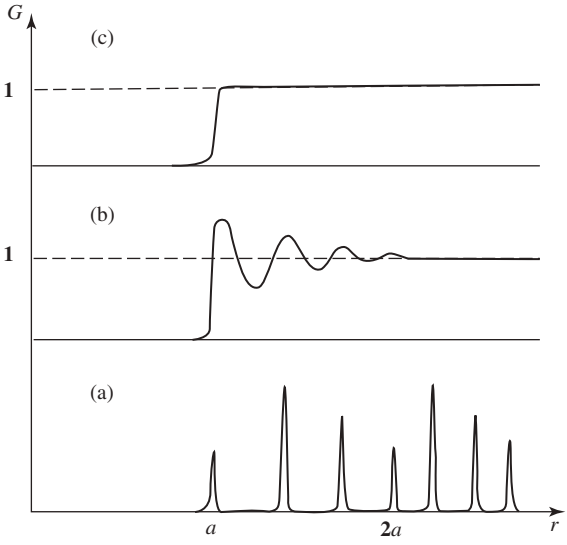

Figure 9.31 A function of the atomic density radial distribution in (a) crystal, (b) liquids and (c) gas.

continuously collapse and new ones are created instead. Each atom in a liquid spends some time τ (referred to as *time of settled life*) in a regular position and makes fluctuations around it. At this time the atoms of a liquid behave like atoms in a crystal. Later, the atom abandons its regular position and jumps to a new position remote from the first by a distance δ approximately equal to the interatomic distance in the liquid. During the jumping process, the atom of a liquid assimilates to a gas atom.

If the temperature decreases, the time of settled life is increased; near the crystallization point this time increases more and the properties of the liquid come nearer to the properties of solids. On the contrary, if the temperature rises, coming nearer to the boiling point, the time of settled life decreases; and the liquid's properties become similar to those of gas.

On melting there is an increase in the specific volume of a substance, on an average by 3%. It is reasonable to assume that the increase in volume is caused by an increase in interatomic distances in the liquid in comparison with that in crystal. However, the compressibility dependence on pressure does not confirm this supposition.

Since there is a short-range order in a liquid the local potential curve $U(x)$ in its nearest surroundings resembles a periodic character (Figure 9.32). Atoms settle down in points of potential energy minimum. In a settled state an atom oscillates with an amplitude significantly smaller than the interatomic distance δ. It was found experimentally that the frequency of these fluctuations have the same order as in solids, namely $v_0 \approx 10^{13}$ sec^{-1}, and the oscillation period $T_0 = (1/v_0) \approx 10^{-13}$ sec. In order to leave the pseudo-equilibrium position an atom should overtake the potential barrier u. The probability of this process is proportional to the Boltzmann factor $e^{-(u/\kappa T)}$. In 1 sec, an atom makes v_0 fluctuations; hence the frequency of jump over to the new position is $v = v_0 \exp(-(u/\kappa T))$. Thus, the time of settled life can be obtained by $\tau = (1 / v) = \tau_0 \exp(u / \kappa T)$

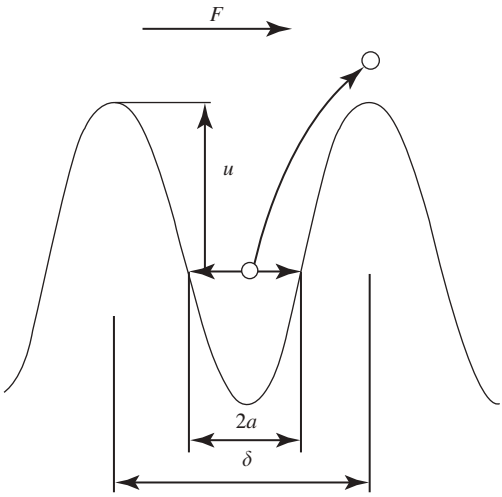

Figure 9.32 Atomic potential curve in a liquid.

When a particle leaves a temporary equilibrium position and occupies a new one, it covers a distance δ. The particle's average speed of wandering (chaotic motion) in liquids is then

$$\upsilon \approx \frac{\delta}{\tau} = \frac{\delta}{\tau_0} \exp\left(-\frac{u}{\kappa T}\right).$$

Suppose that there is a concentration gradient in the liquid. In that case the chaotic wandering creates an excessive atom flow in the direction opposite to the concentration gradient; i.e., diffusion flow will take place. The diffusion coefficient for ideal gases is described by the formula $D = (1/3)\,\lambda\upsilon$, where λ is the molecular free path length, and υ is the average speed of thermal motion (refer to Section 3.3.8). In a liquid the role of free path length is played by the displacement δ and the role of average speed is (δ/τ). Therefore the diffusion coefficient in the liquid can be evaluated as

$$D = \frac{1}{3}\frac{\delta^2}{\tau_0} \exp\left(-\frac{u}{\kappa T}\right). \tag{9.5.2}$$

It can be seen from this expression that *diffusion in a liquid sharply increases with temperature according to the exponential law*. In gases the diffusion coefficient also rises with temperature, but not as fast: under the power $D \propto T^{1/2}$ if heating is isochoric, and as $D \propto T^{3/2}$ if heating is isobaric (see Section 3.7).

Although the expressions obtained are approximate, they usually correctly estimate the order of diffusion coefficient provided that $\delta \approx 10^{-10}$ μm, $v_0 \approx 10^{13}$ sec^{-1} and u (the activation diffusion energy) is approximately equal to the latent heat of melting. The data on diffusion parameters in liquids is given in Table 3.3.

Theoretical treatment of a viscosity phenomenon of liquids can also be carried out proceeding from the same representations. Leaving aside the treatment itself, we write down the final result concerning the temperature dependence of the viscosity as

$$\eta \propto A e^{(u/\kappa T)}, \tag{9.5.3}$$

where A is a pre-exponential factor dependent on the parameters of the liquid and weakly dependent (in comparison with the exponent) on temperature. It can be seen that *liquid viscosity falls very quickly when temperature increases.* The result is not unexpected; such behavior is well known from our everyday experience. It essentially differs from the conclusion that was derived for ideal gas.

The discussion on liquid properties can be used when considering solids. Diffusion in crystals is also defined by the speed of the atom's wanderings, though it is greatly determined by a crystal's imperfections. However, time of settled life in crystals is higher by some order of values than in a liquid because of the fact that practically all crystallographic positions are occupied (see Section 9.4). Atomic hopping (i.e., diffusion) is carried out on those points that are most preferable for this purpose: on vacancies, interstitials, along dislocations and other

places in which the atomic order is destroyed. As a result, the intensity of diffusion in solids is much less than that in liquids. At the same time, the diffusion coefficient also increases exponentially with temperature and in some cases diffusion plays an appreciable role.

Viscosity of solids is extremely high (see Table 3.3). For solids of different nature it differs essentially. It also depends on the structure of substances: degrees of crystallinity, the nature of chemical bonding, etc.

Heat conductivity of solids also changes over a wide range. Similar to gases, the heat conductivity of liquids and crystals depends on their structure, especially of those particles that play the role of energy carriers. In crystals it can be phonons (refer to Section 9.3, in all solids) and electrons (electron gas in metals). As a result, the heat conductivity of solids changes over a wide range (see Table 3.3).

We hope that readers can apply the representations given here to amorphous materials; it should be borne in mind that they have much in common with liquids, but their time characteristics are closer to solids.

Unfortunately, there is no general theory allowing calculation of transport properties of condensed systems. This means that when deciding technical problems based on the use of Fick, Fourier and Newton laws, it is also necessary to use empirical laws and factors. However, it should be remembered that the essence of the phenomena and their physical sense remain the same, as for the description of the elementary model of an ideal gas.

9.6 SOME TECHNICALLY IMPORTANT ELECTRIC PROPERTIES OF SUBSTANCES

Ionic polarization

The mechanisms of polarization are caused by the structure of molecules (previously considered in Chapter 4). There is a type of crystal polarization that has much in common with atomic polarization (refer to Section 4.2.4). In crystals, atoms are in an ordered array. As a result of interaction between neighboring atoms (i.e., chemical bond formation) redistribution of electron density occurs and atoms acquire an effective charge, positive and/or negative. The presence of the two kinds of atomic charge allows one to consider a crystal lattice consisting of two sublattices inserted into one another. Consider for example a crystal structure of cesium chloride (CsCl) (Figure 9.33). Ions Cs^+ and Cl^- form two simple cubic sublattices shifted from each other along a spatial diagonal by a distance equal to half of its length. The total crystal electric dipole moment is zero; the crystal is not polarized. When an electric field is imposed, each sublattice is displaced from the other. The crystal then gets an uncompensated electric dipole moment, i.e., polarization of the whole crystal takes place. Such polarization is referred to as ionic polarization. Elasticity forces will be opposite to the sublattices' displacement; these forces will compensate the action of the electric field. Thus, ionic polarization arises at elastic displacement due to the action of an electric field on positive and negative ions, shifting them from their equilibrium positions. By analogy with atomic polarizability, one can introduce an ionic polarizability with coefficient α_{ion} being attributed to each pair of oppositely charged ions. Under the order of value α_{ion} coincides with the value of α_{at}, i.e., $\alpha_{ion} 10^{-30}$ m^3.

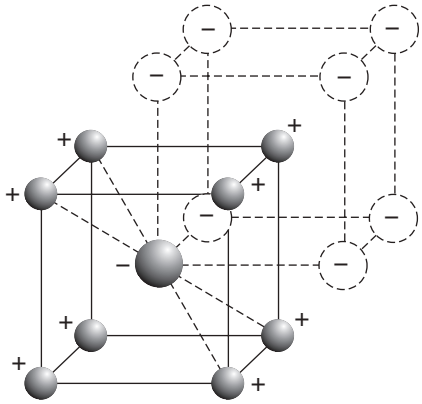

Figure 9.33 Crystal structure of CsCl.

As a result of sublattice displacement, the polarization of an ionic crystal is accompanied by its deformation—the crystal is extended in the direction of the field. This crystal lengthening does not depend on the direction of the field: if the field direction is changed to the opposite direction, it will still lead to the same lengthening of the crystal. Such a change of crystal sizes by the action of the electric field is referred to as *electrostriction*. The relative crystal deformation $\Delta l/l$ depends quadratic on the electric field strength ($\Delta l/l \sim E^2$). The value of the sample length change is very small; for example, for SiO_2 in a field strength $E \sim 10^4$ V/m the relative lengthening of a sample is 10^{-9}.

Currently, normal electrostriction has no practical application. However, there are crystals (e.g., Rochelle salt) in which the positive and negative sublattices are found to be asymmetrically disposed in the crystal; therefore these crystals are polarized even in the absence of an external field. Such polarization is referred to as *spontaneous* (see below).

Charges are formed on the edges of spontaneously polarized crystals, however to measure it one should have a fresh chip. In due course ions of an opposite sign from the surrounding atmosphere neutralize the surface charges and prevent charges being found. When the crystal temperature changes, crystal deformation takes place.

Consider an edge of a crystal on which the bounded positive charge exists; they are compensated by adsorbed negative ions. With an increase in temperature, crystal polarization will also increase leading to an increase in the density of the bounded charges, and adsorbed negative ions will no longer compensate them. Hence, a positive charge will be spread on this surface. Similarly, the negative charge will be concentrated on the opposite edge. Thus, the potential difference appears at heating between crystal sides. The phenomenon of the occurrence of electric charges on the edges of a crystal with a change in its temperature is referred to as a *pyroelectric effect*.

A piezoelectric effect

This effect exhibits the presence of spontaneous polarization of a crystal. G. Curie and P. Curie found that at mechanical compression or stretching of some crystals, the electric charges appeared on their edges. This phenomenon is referred to as a *direct piezoelectric*

effect. Later, the opposite effect was also found experimentally, i.e., a *reversed piezoelectric effect* that consists of crystal deformation by applying an external electric field. At reversed piezoelectric effect, unlike electrostriction, the relative deformation of a crystal $\Delta l/l$ depends linearly on the intensity of an electric field ($\Delta l/l \sim E$); consequently, if the crystal is extended in some direction of the electric field, the crystal will be compressed in the opposite field direction. In this case, the relative deformation of the crystal is by some order of values larger than at electrostriction.

The piezoelectric effect is observed in noncentosymmetric crystals and is especially great in quartz, tourmaline, Rochelle salt, barium titanate, sugar, blende, and in some others. The most important at present is quartz, which has found wide application in practice, for example, in the widely known lighters.

Consider the nature of the piezoelectric properties of quartz, SiO_2. In this crystal the silicon atom bears a positive charge and the oxygen atom a negative charge. A freely grown quartz crystal represents a hexahedron prism topped with many-sided prisms (Figure 9.34). The axis of the prism Oz is an optical crystal axis. Directions Ox_1, Ox_2 and Ox_3 are electric axes of the crystal; apparently all of them are equivalent. If one cuts out a quartz plate perpendicularly to the optical axis and compresses it along one of the electric axes, bounded charges will appear on the surface of the plate. On stretching, the signs of the charges change to its opposite. On compression or stretching along the optical axis Oz, a piezoelectric effect usually does not appear.

Let us find the mechanism by which charges occur on crystal surfaces on deformation. The hexagonal atomic crystal structure is shown in Figure 9.35a where silicon atoms are

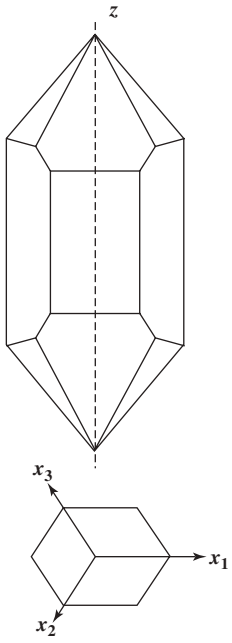

Figure 9.34 Crystal forms of SiO_2 single crystal.

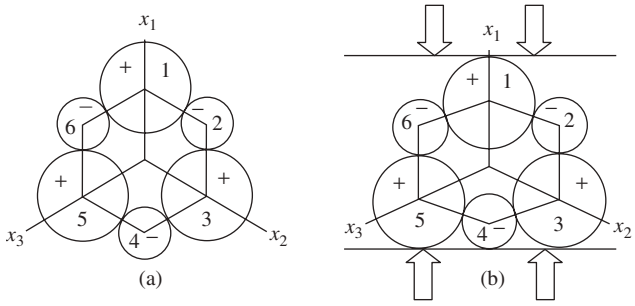

Figure 9.35 A scheme of disposition of positive (Si) and negative (O) atoms in: (a) a free crystal; (b) a forced crystal.

designated by a "+" sign and oxygen atoms are designated by a "−" sign. If the crystal is compressed in the direction of one of the electric axes (Figure 9.35b) the Si_1 ion will be wedged between ions O_2 and O_6 and the O_4 ion will be wedged between Si_3 and Si_5 ions. Since in the absence of electric voltage, all charges compensate each other, the introduction of a positive charge of the Si_1 ion creates an excessive negative charge on the edge of the crystal, and the displacement of the O_4 ion creates an excessive positive charge. Hence, a negative-bounded charge appears on the top surface of the crystal and a positive charge appears on the bottom. On stretching, the signs of the charges will be opposite.

The reverse piezoelectric effect can be similarly explained. On bringing a quartz plate into an electric field, it will be deformed due to displacement of the charges; the sign on deformation changes to the opposite when the direction of the field is changed.

Direct and reverse piezoelectric effects have found very wide application in practice: for measuring pressure in rapidly proceeding processes, for transformation of electric vibrations in mechanical and in acoustoelectronics, etc.

Ferroelectricity

There are substances among dielectrics whose dielectric permeability ε in a narrow temperature interval is extremely high ($\sim 10^3 - 10^4$) and depends nonlinearly on the electric field strength E. Such crystals are referred to as *ferroelectrics;* the Rochelle salt $NaKC_4H_4O_6{\cdot}4H_2O$ was the first to be discovered in the series by I.V. Kurchatov in the last century. A condenser with such dielectrics between plates has various capacitances, depending on the potential difference applied. The dependence of the polarization $\Re$ from the value of the electric field strength is given in Figure 9.36. Before application of an electric field, the ferroelectric is not polarized, i.e., $\Re = 0$ (point O). During the process of increasing the electric strength, the polarization changes according to curve ABC. If we now begin to reduce the strength E, the polarization decreases not along the previous curve CBOA, but along curve CBE. When the field strength falls to zero, the polarization appears to be $\Re_r$.This polarization value is referred to as *residual ferroelectric polarization*.

If the field is changed to the opposite direction and increased, it reduces polarization and at $E = E_F$ the ferroelectric polarization will vanish to zero. The value of the residual field that removes ferroelectric polarization E_F is referred to as a coercive force. With a further

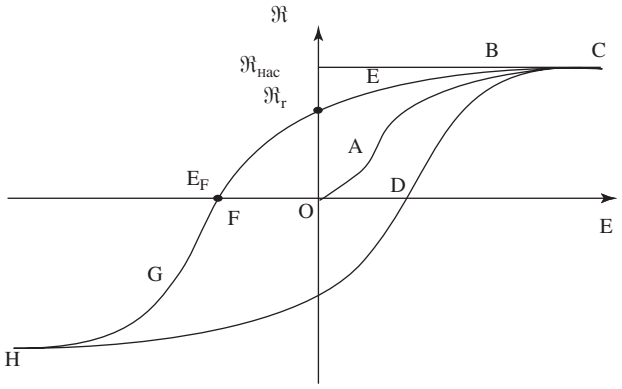

Figure 9.36 A hysteresis loop in ferroelectrics.

field increase the polarization changes along the curve FGH. If after point H, the field strength E again starts increasing in a positive direction to axis E, the polarization will change along the curve HDC. Thus, Figure 9.36 shows that the ferroelectric polarization change detains from the change of the polarizing field. This phenomenon is referred to as hysteresis and the whole closed curve is a *hysteresis loop* (similar to ferromagnetics). In general polarization, decreases with temperature, and ferroelectricity absolutely disappears at a temperature called the *Curie point* T_C; the crystal transforms to a paraelectric state.

The phenomena of magnetization/polarization in ferromagnetics and ferroelectrics have much in common. In the Russian literature, however, another definition is used, i.e., segnetoelectrics, in accordance with the name of the first-discovered compound of that type. Rochelle salt in Russian is called segnetova salt. The phenomenon was discovered by I.V. Kurchatov in 1932.

There are many ferroelectric crystals with the common formula ABO_3, natural and synthesized, on the basis of the first-discovered perovskite mineral $CaTiO_3$ (Figure 9.37).

All constituent atoms can be isomorphic substituted, both in hetero- or homovalence manner, the resulting compound possessing ferroelectric properties. In the paraelectric phase of these crystals, ions of small size (type B, black balls) are in the centers of ideal oxygen octahedrons. At temperatures lower than T_C, due to specificity of interatomic interaction and features of atomic thermal vibration, some ions are displaced from their ideal positions, the structure becoming noncentrosymmetric. The ion of type B (or A) can displace along one of three symmetry axes—the second, third and fourth orders. Any of these displacements leads to the occurrence of a spontaneous dipole moment. This takes place simultaneously in a certain area of the crystal. Such areas with a certain macroscopic volume of spontaneous polarization are called *domains*.

If the ferroelectric is not polarized as a whole, the distribution of the domains is random. When an external electric field is imposed the domains turn gradually along the field. Saturation is reached at large fields: all dipole moments of all domains are turned in one direction. Indeed, the picture is quite similar to that described in Section 5.3, which is devoted to ferromagnetism.

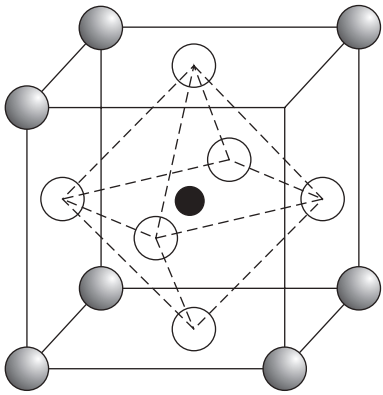

Figure 9.37 A crystal type of perovskite $CaTiO_3$.

All ferroelectrics are also piezoelectrics; therefore they have found wide application in sound and ultrasonic generators, microphones, ceramic condensers, etc.

Electrets

There are some dielectrics which, in the absence of an external electric field, can preserve the polarized state for a long time. These are referred to as electrets. An example of such a compound is wax, which consists of long molecules with a permanent electric dipole moment. If a small amount of wax is melted and, while it is not yet hardened, is placed in a strong electric field, the wax molecules will partly be oriented by the guidance given along the field; the wax remains in polarized state after it has hardened. Organic dielectrics possess the same property as well (naphthalene, paraffin, ebonite, mica, nylon, etc) and inorganic dielectrics (sulfur, boric glass, titanates of alkali earth materials of the perovskite type, etc.). Electrets are analogs to permanent magnets. They can be produced both as described above (thermoelectrets), or by the action of light on a photoconducting dielectric by the action of a strong electric field (photoelectrets). All electrets have a stable surface charge σ ,$\sim$ 100 μC/m^2. The time of an electret's life, i.e., the time for which the surface charge will decrease in e time, lasts from several days to many years.

Electrets are used as sources of a permanent electric field. They are also used in radio engineering (microphones and phones), in dose metering (electret dosimeters), in measuring techniques (electrostatic voltmeters), in computer facilities (memory elements), etc.

Liquid crystals

In modern techniques the so-called *liquid crystals* are gaining increasing importance. The liquid crystal state is characterized as being an intermediate between isotropic liquids and anisotropic solids: in some temperature interval they preserve some properties of a liquid (e.g., fluidity) and some properties of a crystal (e.g., anisotropy). The liquid crystal state is realized more often in substances whose molecules consist of a long flat atomic structure (rods) with included benzene rings (e.g., 4-met-oksi-benziliden-4′-butil-aniline). Properties of liquid crystals are defined by different features of molecular packing in

domains: they are built usually by the long axis along a single direction; whereas azimuthal orientation in different substances can behave differently.

Depending on the molecular properties (e.g., the presence of dipole moments and orientation), the existence of the short- or long-range ordering in a molecule arrangement (refer to Section 9.5) and specificities of intermolecular interaction liquid crystals possess the whole scale of macroscopic properties. Practically all liquid crystals are dielectrics with strong anisotropy of electric properties, i.e., their dielectric permeability depends on direction (there are at least two value of ε : $\varepsilon_{\perp}$and $\varepsilon_{\parallel}$). In an external electric field the liquid crystal molecules are oriented in such a way that the direction of the maximum dielectric permeability coincides with the external field direction.

Almost all liquid crystals are diamagnetic. An exception is made with those substances whose molecules incorporate free radicals with permanent magnetic moments. Anisotropy of electric and optical properties of the liquid crystals, closely connected with anisotropy of their molecular structure, causes variety of their electrooptical properties. The external electric field can render a very strong influence on optical properties of liquid crystals, changing, for instance, their transparency and color. Therefore they have found very wide application as electronic indicator panel in microelectronics (calculators, watches and other devices). Such types of devices require very low voltage (parts of volts) and power (μW).

In some cases optical properties of liquid crystals depend very strongly on temperature. Substances possessing such properties find application, for example, in industry and in medicine (for diagnostics of deviation from normal of the thermal mode of body parts).

PROBLEMS/TASKS

9.1. A crystal lattice is depicted in Figure T9.1. Find the Miller indexes of the crystallographic direction given in bold.

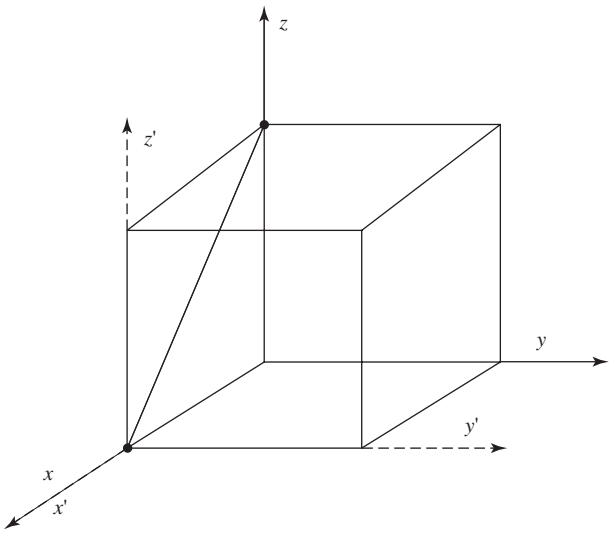

9.2. A crystal lattice is depicted in Figure 9.5e. Find its Miller indexes.
9.3. Using the free electron model, calculate the maximum electron's velocity in a potassium metal at $T = 0$ K assuming the Fermi energy $\varepsilon_F = 2.02$ eV (see Example E9.5) and corresponding electron's momentum p_F.
9.4. Two nanoparticles with linear particle dimensions $L_1 = 10a$ and $L_2 = 20a$ (a is the lattice period) are at the same temperature $T = \theta_D/100$, where θ_D is the Debye temperature. Calculate the ratio of the internal energy U_2/U_1 for the case of the same amount of atoms (the zero energy can be neglected).
9.5. Two nanoparticles with linear particle dimensions $L = 10a$ and $= 20a$ (a is the lattice period) are at the same temperature $T = \theta_D/100$, where θ_D is the Debye temperature. Calculate the ratio of heat capacities $C_2(T)/C_1(T)$ for the case of the same amount of atoms (the zero energy can be neglected).
9.6. A nanoparticle with linear particle dimensions $L = 10\ a$ (a is the lattice period) is heated from temperature $T = \theta_D/100$ up to $T_2 = \theta_D/50$, where θ_D is the Debye temperature. Calculate the ratio of the internal energies $U_2(T_2)/U_1(T_1)$ and compare the ratio with that of bulk crystal $U_\infty(T_2)/U_\infty(T_1)$. (The zero energy can be neglected.)
9.7. Nanoparticles with linear dimensions $L = 10a$ and $= 20a$ (a is the lattice period) are heated (in average) from temperature $T_1 = \theta_D/100$ to $T_2 = \theta_D/50$ (θ_D is the Debye temperature). Determine how much its heat capacity will change $C(T_2)/C(T_1)$. Compare the result obtained with the analogous ratio $C_\infty(T_2)/C_\infty(T_1)$ for bulk crystal.
9.8. Determine how much a nanoparticle's heat capacity at temperature $T = \theta_D/100$ (θ_D is the Debye temperature) with linear dimensions $L = 10a$ (a is the lattice period) differs from that of C_∞ of the same bulk crystal after converting to an equal number of atoms.
9.9. There are nanoparticles with linear dimensions $L_1 = 10a$ (a is the lattice period) and $L_2 = 20a$ of the same composition and temperature ($T = \theta_D/100$). Estimate the ratio of heat transfer coefficients κ_1/κ_2 of nanomaterials ($\kappa = (1/3)C\upsilon\lambda$, C_V being the heat capacity and υ is an averaged sound speed; assume that the free path λ in the nanoparticles is limited by particle dimensions L.
9.10. How many times larger is the ratio of free electrons to one metal atom at $T = 0$ K in aluminum than in copper. The Fermi energy of these two metals is $\varepsilon_{F,Al} = 11.7$ eV and $\varepsilon_{F,Cu} = 7.0$ eV.
9.11. A nanoparticle with linear dimensions $L = 10a$ (a is the lattice period) is heated from a temperature $T_1 = \theta_D/100$ up to $T_2 = \theta_D / 50$, where θ_D is the Debye temperature. Calculate the internal energies ratio $U_2(T_2) / U_1(T_1)$ and compare the ratio with that of bulk crystal (the zero energy can be neglected).

ANSWERS

9.1. Indexes are $[-1,0,1]$.
9.2. Indexes are $(1,2,-1)$.
9.3. $\upsilon_{max} = \sqrt{2\varepsilon_F / m} = 8.42 \times 10^5$ m/sec^2 and $p_F = 9.11 \times 10^{-31} \cdot 8.42 \times 10^5 = 7.67 \times 10^{-25}$ kg m/sec.

9.4. $(U_2/U_1) = 26.2$.

9.5. $(C_2/C_1) = 16.2$.

9.6. $[U_{2N}(T_2)/U_{1N}(T_1)] = 405$ and $[U_\infty(T_2)/U_\infty(T_1)] = 8$.

9.7. $[C(T_2)/C(T_1)] = 130$, $[C_\infty(T_2)/C_\infty(T_1)] = 8$.

9.8. $(C_\infty/C_N) = 41.5$.

9.9. $(\kappa_1/\kappa_2) = 0.03$.

9.10. Three times.

9.11. $[U_2(T_2)/U_1(T_1)]_N = 405$, $[U_2(T_2)/U_1(T_1)]_\infty = 16$.

This page intentionally left blank